

UNCLASSIFIED

AD NUMBER
ADB000283
NEW LIMITATION CHANGE
TO Approved for public release, distribution unlimited
FROM Distribution authorized to U.S. Gov't. agencies only; Test and Evaluation; 16 JAN 1974. Other requests shall be referred to Chief Office of Naval Research, Attn: Code 102-OSC, Arlington, VA 22217.
AUTHORITY
CNO [N772] ltr N772A/6U875630, 20 Jan 2006 and ONR ltr 31 Jan 2006

THIS PAGE IS UNCLASSIFIED

AD B 0 0 2 8 3

# THE UNIVERSITY OF TEXAS AT AUSTIN

ARL-TM-73-42  
20 December 1973

Copy No.

## QUALITY CONTROL ANALYSIS OF SUS PROCESSING FROM ACODAC DATA

Stephen K. Mitchell and Terry D. Plemons

OFFICE OF NAVAL RESEARCH  
Contract N00014-70-A-0166, Task 0016



Best Available Copy

AD B 0  
DEC 5  
R  
E

DISTRIBUTION LIMITED TO U. S. GOVERNMENT AGENCIES  
ONLY, TEST AND EVALUATION; 16 JANUARY 1974.  
REQUESTS FOR THIS DOCUMENT MUST BE REFERRED TO THE  
OFFICE OF NAVAL RESEARCH, CODE 102-05C.

ARL-TM-73-42

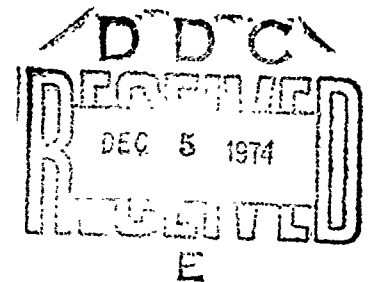
QUALITY CONTROL ANALYSIS OF SUS PROCESSING FROM ACODAC DATA

Stephen K. Mitchell and Terry D. Plemons

20 December 1973

First Revision: 16 January 1974  
Second Revision: 4 March 1974  
Third Revision: 15 October 1974

OFFICE OF NAVAL RESEARCH  
Contract N00014-70-A-0166, Task 0016



APPLIED RESEARCH LABORATORIES  
THE UNIVERSITY OF TEXAS AT AUSTIN  
AUSTIN, TEXAS 78712

DISTRIBUTION LIMITED TO U. S. GOVERNMENT AGENCIES  
ONLY, TEST AND EVALUATION; 16 JANUARY 1974.  
REQUESTS FOR THIS DOCUMENT MUST BE REFERRED TO THE  
OFFICE OF NAVAL RESEARCH, CODE 102-OSC.

## ABSTRACT

The errors associated with the analysis of acoustic signals generated by underwater explosive sources are analyzed in this report. Thus, the effects of analog reproduction and subsequent digital conversion of the data on the estimation of propagation loss are considered. In addition the techniques of the spectral analysis as applied to these data are discussed. It is shown that the digitizing processing can be repeated on a day-to-day basis to the extent that the energy in frequency bands for either shots or noise have standard deviations of 1 to 2%. The times at which the automatic shot processor detected a shot showed no fluctuations other than those to be expected from the temporal resolution imposed by the sampling rate. The standard deviations due to repeated processing of transmission loss for a given frequency band is of the order of 0.1 to 0.2 dB.

## TABLE OF CONTENTS

	<u>Page</u>
ABSTRACT	iii
I. INTRODUCTION	1
II. EFFECTS OF TAPE PLAYBACK AND ANALOG-TO-DIGITAL CONVERSION UPON SHOT PROCESSOR	3
III. EFFECTS OF METHODS OF DIGITAL SIGNAL COMBINATION ON SHOT SPECTRAL ANALYSIS	13
A. Theoretical Description of Digital Spectral Analysis	14
B. Effects of Data Segment Length on Digital Signal Summation	18
C. Comparison of Methods of Digital Signal Summation	30
IV. EFFECTS OF SAMPLING WITHOUT PHASE CONTROL	37
V. STABILITY OF CALIBRATION SIGNAL AS A FUNCTION OF TIME	41
VI. SUMMARY	43

## I. INTRODUCTION

This memorandum gives the results of investigations conducted to obtain measurements of errors associated with various components of the processing system used at Applied Research Laboratories, The University of Texas at Austin, for the analysis of ACODAC analog data. The significant components of the analysis procedure are investigated individually to determine the magnitude of error that each contributes to the final estimate of ambient noise level and propagation loss. The areas considered in the following sections are (1) the consistency of the analog-to-digital conversion and shot processing, (2) the spectral analysis methods used to determine the energy content of acoustic signals in selected frequency bands, (3) the effects of sampling without phase control, and (4) the stability of the ACODAC calibration signal as a function of time. The concluding remarks are made in Section VI.

## II. EFFECTS OF TAPE PLAYBACK AND ANALOG-TO-DIGITAL CONVERSION UPON SHOT PROCESSOR

To examine the effects of analog tape playback and analog-to-digital conversion of ACODAC data upon the shot processor, a segment of data was subjected to repeated digitization and analysis.

A 1 h segment of ACODAC recording of the CHURCH ANCHOR exercise was selected; the data record contained approximately 30 shots plus one calibration signal sequence. Typical envelopes of the 800 ft, 300 ft, and 60 ft shots are shown in Fig. 1. On three different days, the same 1 h segment of recorded data was digitized five times for a total of 15 digitized records. These were regarded as an ensemble of noise corrupted signals; the noise in this case was due to fluctuations introduced by the playback system. The digitized records were then processed with the ARL shot processor, which automatically detects a shot and then does spectral analysis of the shot and of a segment of ambient noise preceding it. The processor output record includes the energy of the shot and the noise in six frequency bands ( $1/3$  octave centered at 12.5, 25, 50, 100, 160, and 200 Hz); these are used to compute transmission loss.

For each shot, the mean and standard deviation of the computed energies were estimated; these statistics were calculated for each day (groups of 5 digitizations) as well as for the ensemble of 15.

As an example, consider the 50 Hz band of the signals received on hydrophone 4 from shots detonated at nominal depths of 60 ft. During day 21, hour 23 (20 December 1972, 1100) of the exercise, the Bartlett was approximately 500 nm from station A; the 60 ft shot arrived approximately 20 sec into the 13th, 18th, 23rd, etc., min.

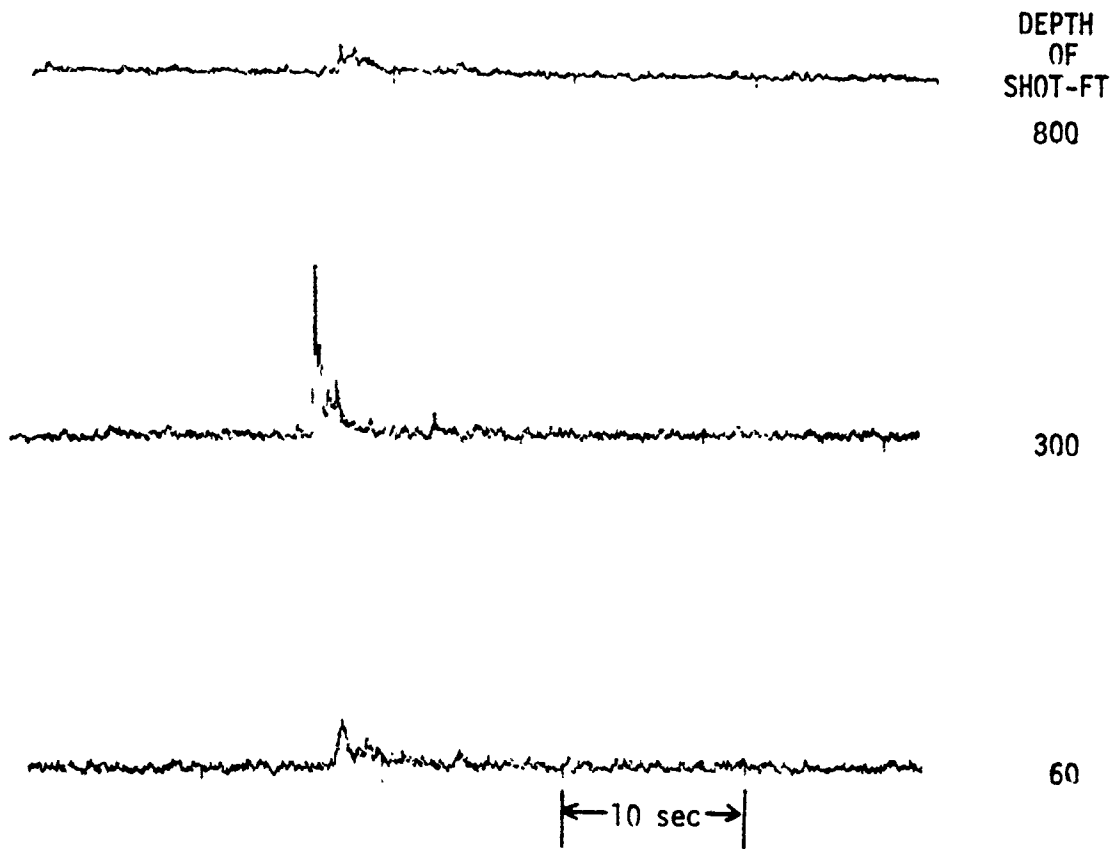


FIGURE 1  
REPRESENTATIVE RECEIVED SHOT  
SIGNALS FROM ACODAC HYDROPHONE 4  
20 DEC 1972, 1126: CHURCH ANCHOR



In Fig. 2 the energy  $(S+N)$  averaged over the 5 digitizations per day is plotted for the digitization days versus minute of reception; the energy scale is in arbitrary units, and the calibration signals have not been taken into account for this figure. The largest standard deviation among the digitization sequences on a particular day for a given shot was 0.032 units, about the size of the solid dot symbols. This figure serves mainly to point up the possible variation from day to day of the level reproduced from a given recording. The shot detonation depths as provided by Underwater Systems, Inc.,\* are also shown on Fig. 2.

Figure 3 shows daily averages for each of the 3 digitization days of  $10 \text{ Log}(S+N-\hat{N})^{**}$  minus  $10 \text{ Log}(\text{Calibration})$  versus time. Except for source level and hydrophone sensitivity compensation, this is effectively transmission loss. Though at most times the differences are scarcely perceptible, at minute 18 there is an almost 0.2 dB spread. The standard deviation of transmission loss for individual shots was 0.07 to 0.15 dB. As may be seen proper use of the calibration signal removes the spread which might be anticipated from Fig. 2. The signal-to-noise ratios of the signals used to compute Fig. 3 are shown in Fig. 4.

The 300 ft shot was detonated 1 min before the 60 ft shot. Figures 5 and 6 show transmission loss curves similar to Fig. 3 for the 300 ft shot in the 50 Hz and 200 Hz frequency bands (absolute level comparison between Fig. 3 and Figs. 5 and 6 should not be made). The small effect of system variability upon transmission loss shown by Figs. 3, 5, and 6 was typical of results from all frequencies and depths. Also typical is the variability of energy levels occurring between closely spaced shots.

---

\* "SUS Shot Statistics," paper tape records mailed to ARL on 12 November 1973.

\*\* $\hat{N}$  is the noise energy level estimated from a portion of the record preceding the time of detection.

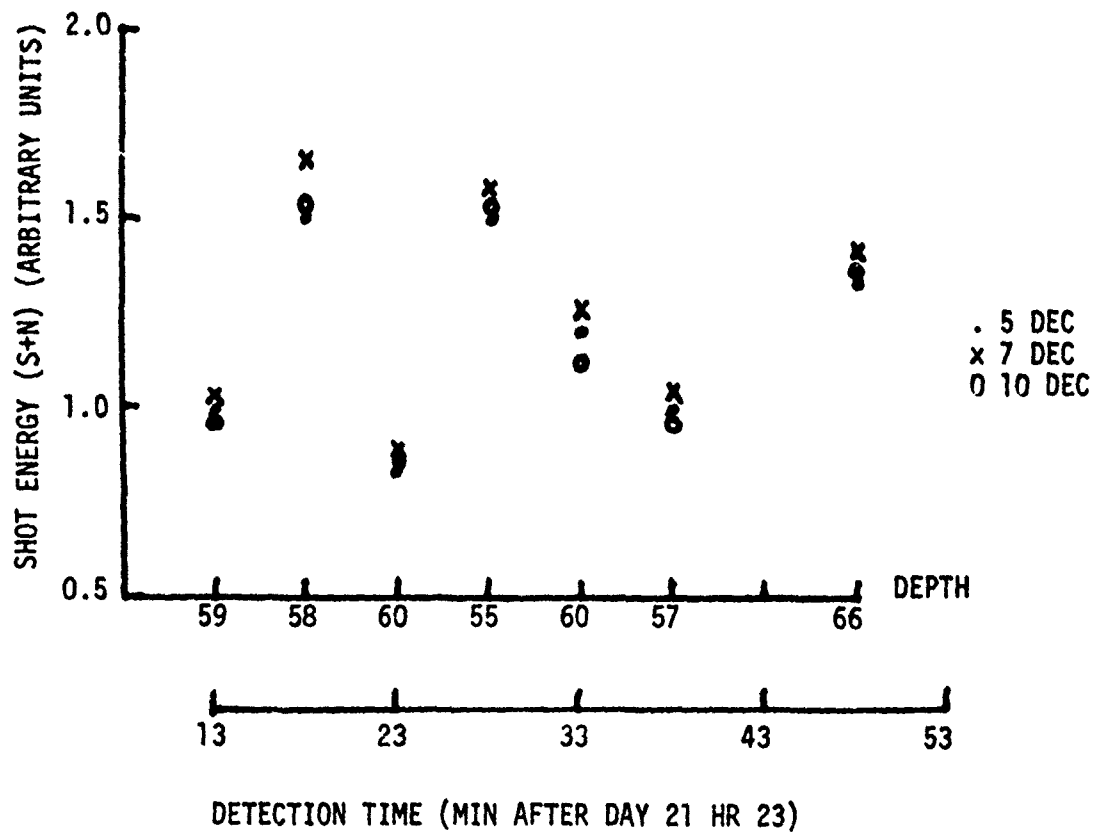


FIGURE 2  
 AVERAGE SHOT ENERGY COMPUTED FROM  
 DATA DIGITIZED ON THREE DIFFERENT DAYS  
 HYDROPHONE 4, SIGNAL PLUS NOISE  
 FREQUENCY BAND: 1/3 OCTAVE CENTERED AT 50 Hz

AS-74-367

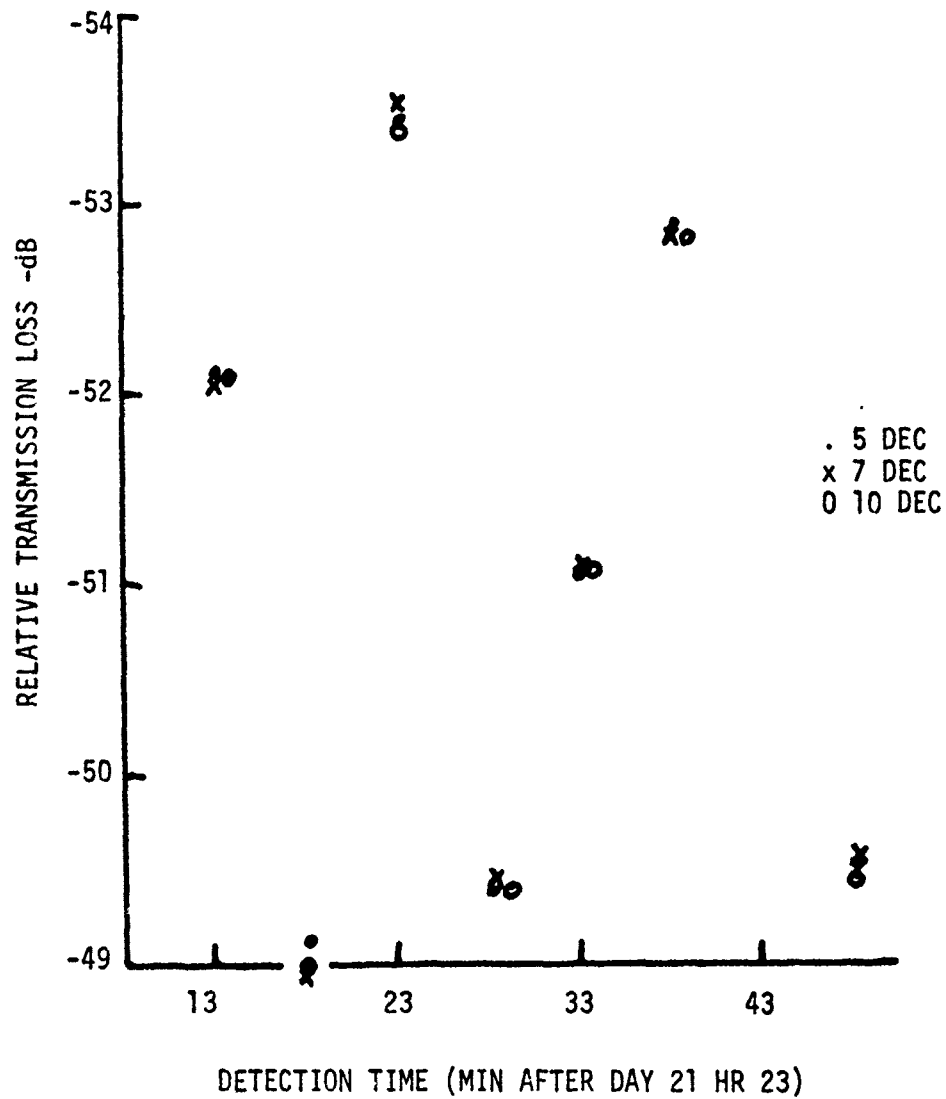


FIGURE 3

RELATIVE TRANSMISSION LOSS COMPUTED FROM  
DATA DIGITIZED ON THREE DIFFERENT DAYS

DEPTH OF SHOT = 60 ft

FREQUENCY BAND: 1/3 OCTAVE CENTERED AT 50 Hz

PLOTTED POINTS ARE  $10 \log(\text{SIGNAL-NOISE}) - 10 \log(\text{CALIBRATION SIGNAL})$   
HYDROPHONE 4

AS-74-368

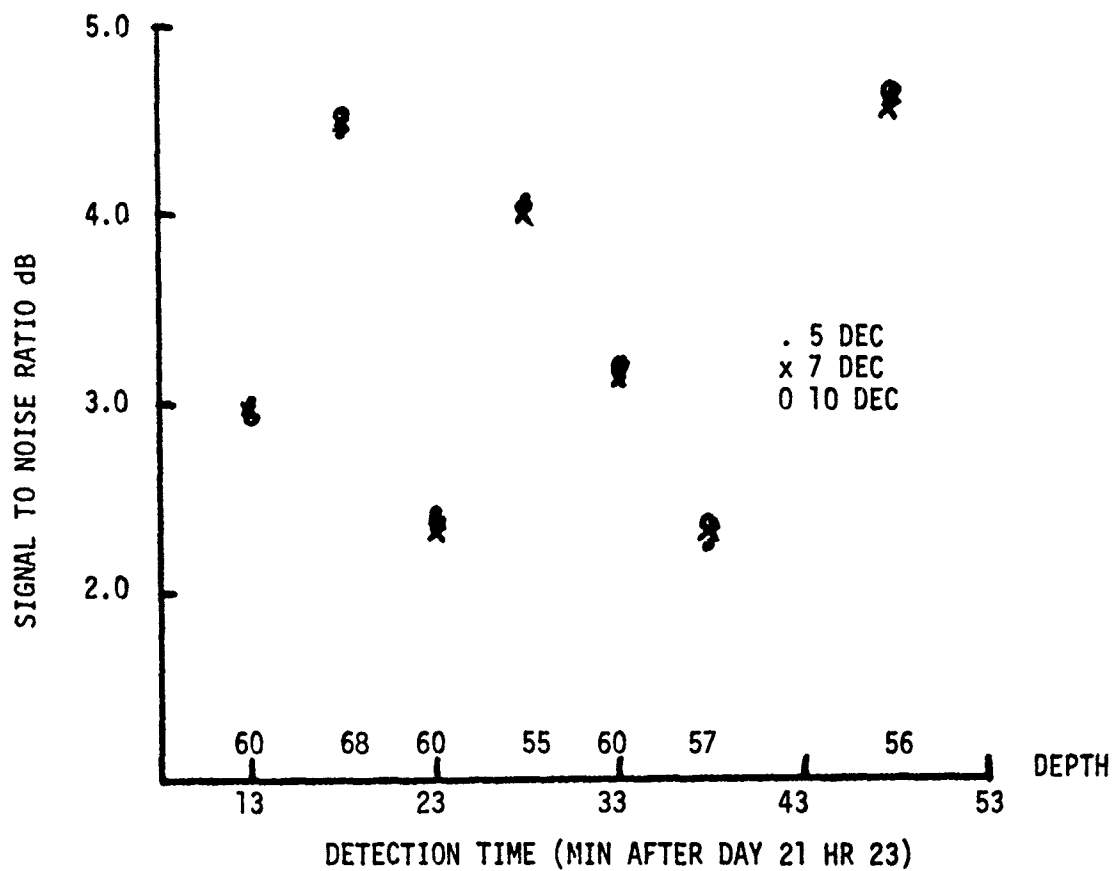


FIGURE 4

AVERAGE SIGNAL TO NOISE RATIO COMPUTED  
 FROM DATA DIGITIZED ON THREE DIFFERENT DAYS  
 $SIGNAL\ TO\ NOISE\ RATIO = 10 \log[(S+N)/N]$   
 FREQUENCY BAND: 1/3 OCTAVE CENTERED AT 50 Hz  
 HYDROPHONE 4

AS-74-369

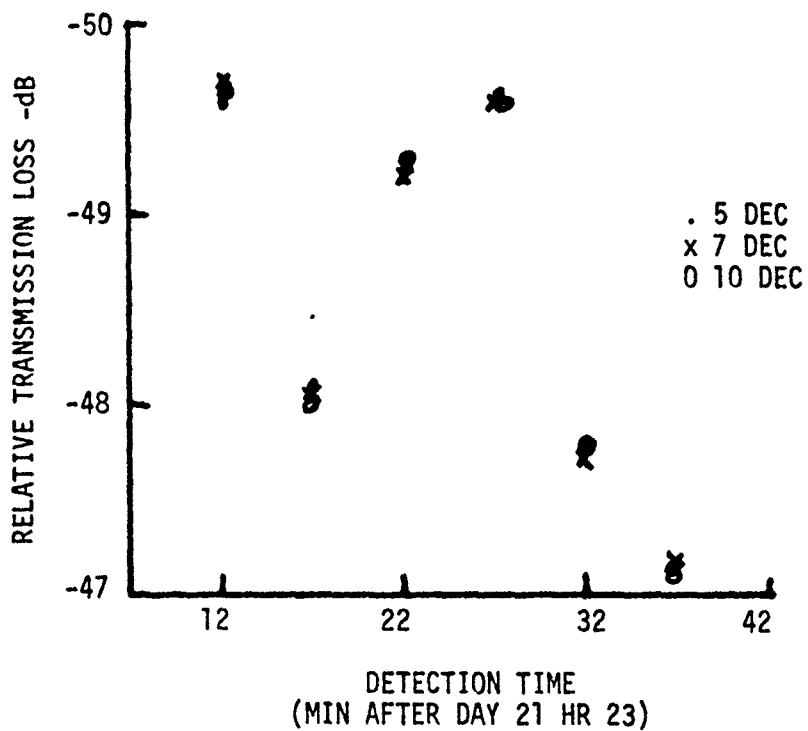


FIGURE 5  
 RELATIVE TRANSMISSION LOSS COMPUTED  
 FROM DATA DIGITIZED ON THREE DIFFERENT DAYS  
 DEPTH OF SHOT = 300 ft  
 $TRANSMISSION\ LOSS = 10\ LOG(SIGNAL-NOISE) - 10\ LOG(CALIBRATION\ SIGNAL)$   
 FREQUENCY BAND = 1/3 OCTAVE CENTERED AT 50 Hz

AS-74-370

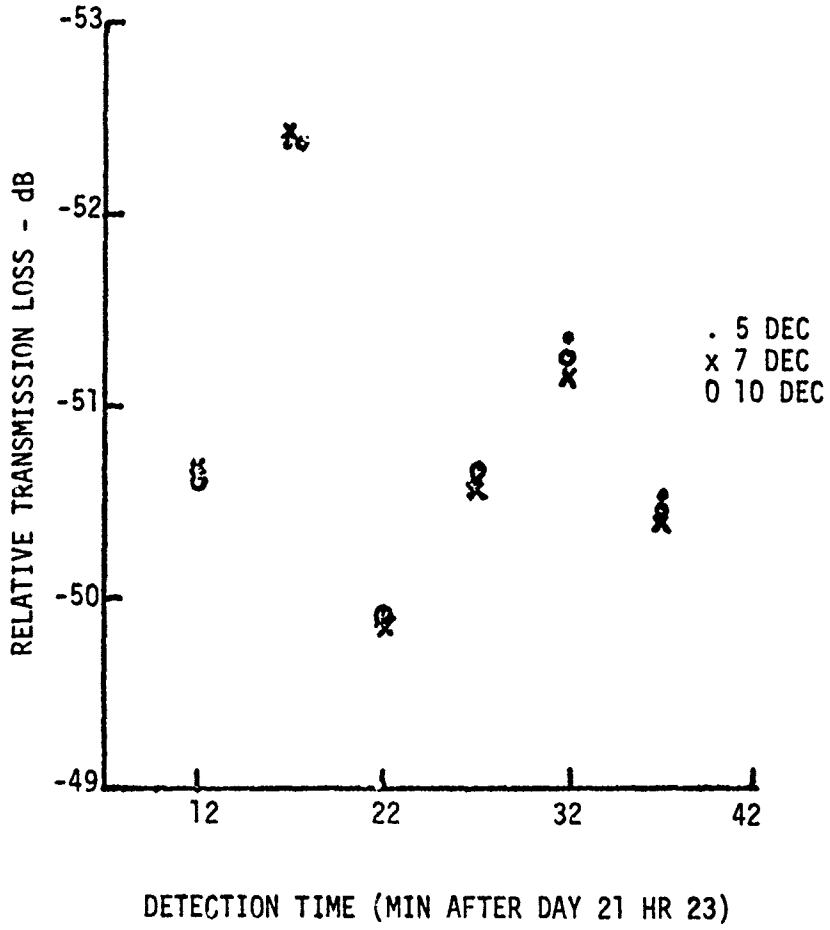


FIGURE 6

RELATIVE TRANSMISSION LOSS COMPUTED FROM  
DATA DIGITIZED ON THREE DIFFERENT DAYS

DEPTH OF SHOT = 300 ft

TRANSMISSION LOSS =  $10 \text{ LOG}(\text{SIGNAL-NOISE}) - 10 \text{ LOG}(\text{CALIBRATION SIGNAL})$

FREQUENCY BAND = 1/3 OCTAVE CENTERED AT 200 Hz

AS-74-371

Examination of the statistics from all hydrophones and bands showed the following.

1. On a single day, the energy in the frequency bands for either shots or noise had standard deviations of 1% to 2%. The energy in the same bands of the calibration signals showed a similar spread.

2. The signal levels as digitized showed variations from day to day which yielded 5% to 10% ( $5\% \approx 0.2$  dB) deviations of energy in the bands before the calibration signal was used for compensation. This day-to-day variation was of the nature of a daily change in overall playback gain, though it likely is due to variations in the analog tape/playback head combination; the entire 1 h record, including calibration signals, was similarly affected, thus allowing compensation to be made.

3. The times at which the automatic shot processor detected a shot showed no fluctuations other than those to be expected from the temporal resolution imposed by the sampling rate. The standard deviations of detection times for individual shots were in the range 5 msec to 20 msec. The data sampling rate was 600 Hz, but only every fourth sample was considered for detection; from this, one should expect an rms jitter of 13 msec.

4. The standard deviations of transmission loss for a given frequency band is of the order of 0.1 to 0.2 dB.

### III. EFFECTS OF METHODS OF DIGITAL SIGNAL COMBINATION ON SHOT SPECTRAL ANALYSIS

This section provides detailed descriptions of digital techniques used for estimating the energy of the shot in selected frequency bands. The current goal of the analysis program is that shot energy measurements presented for one-third octave bands obtained by digital analysis techniques be compatible with measurements previously made using analog techniques. Digital analysis methods are concerned with two practical realities.

1. The typical received shots analyzed in the LRAPP experiment can have time durations of 30 sec or 1800 samples at a sample rate of 600 Hz. (Durations up 3 to 4 times this length have been observed.) A single Fourier transformation of this length is not practical with most computer capabilities. This necessitates segmenting the shot record into manageable, contiguous segments whose Fourier transforms are easily computed. This process, then, presents the second problem.

2. The individual Fourier transforms must be summed in some manner to give the final power spectrum of the shot in a given one-third octave frequency band. The summation can be made using the complex components, where the phase information of the Fourier transforms of the contiguous segments is preserved, or the summation can be made using the energies, where the magnitudes of the individual spectra are preserved.

In this section, a detailed description of these two techniques is given. First the theoretical aspects of the problem are considered.



A. Theoretical Description of Digital Spectral Analysis

Consider a time function  $\tilde{x}(t)^*$  defined over the interval  $(0, T)$ .  
The Fourier transform of  $\tilde{x}(t)$  is

$$F(f) \equiv \mathcal{F}\{\tilde{x}(t)\} = \int_{-\infty}^{\infty} \tilde{x}(t) e^{-i\omega t} dt \quad , \quad (1)$$

where  $\omega = 2\pi f$ . Since  $x(t)$  is nonzero only over the interval  $(0, T)$

$$\tilde{F}(f) = \int_0^T \tilde{x}(t) e^{-i\omega t} dt \quad . \quad (2)$$

The spectral intensity density of  $x(t)$  is

$$\tilde{W}(f) = |\tilde{F}(f)|^2 \quad . \quad (3)$$

The total energy in the signal is

$$\tilde{E} = \int_0^T \tilde{x}^2(t) dt \quad , \quad (4)$$

which is also available from the spectral density

$$\tilde{E} = \int_{-\infty}^{\infty} \tilde{W}(f) df \quad . \quad (5)$$

---

\* Tilde used to denote continuous representation.

The energy in a selected frequency band  $(f_1, f_2)$  is

$$\tilde{E}_{12} = 2 \int_{f_1}^{f_2} \tilde{W}(f) df \quad . \quad (6)$$

The analog to Eq. (2) for discrete processing is

$$F_j = W \sum_{m=0}^{K-1} x_m e^{-(2\pi i j m / k)} \quad . \quad (7)$$

where

$$x_m = \tilde{x}(m\Delta t), m\Delta t \in [0, T] \quad .$$

$W$  is a weighting factor to preserve Parseval's relation (Eqs. 4 and 5).

It is well known that

$$F_j = \sum_{m=-\infty}^{\infty} \tilde{F}(f_m)$$

where  $f_m = (j + Km) / \Delta t$ . If the sample rate is adequate,

$$\tilde{F}(f_m) \approx 0 \quad , \quad m \neq 0$$

so that

$$F_j \approx \tilde{F}(j/\Delta t) \quad .$$

Analogous to Eq. 6, the energy in a frequency interval  $[f_1, f_2]$  is defined as

$$E_{12} = 2 \sum_{j=j_1}^{j_2} |F_j|^2 .$$

A practical limitation to the computing of Eq. 7 is the size of available computer storage. To maintain reasonable data sample length it will at times be necessary to obtain the spectral energy in the frequency bands of interest by transforming segments of the data and then accumulating the transformation of the segments.

Let us assume that the time interval of the signal has been broken into  $N$  segments of length  $L$ ;  $L=K/N$ . We define

$$x_m^l = x_{m+lL} \quad ; \quad \begin{array}{l} l = 0, 1, \dots, N-1 \\ m = 0, 1, \dots, L-1 \end{array}$$

and

$$F_j^l = W \sum_{m=0}^{L-1} x_m^l e^{-(2\pi i j m / L)} \quad , \quad j = 0, 1, \dots, L^{-1} .$$

The spectral energy density at frequency  $j/\Delta t$  for the signal in interval  $l$  would be

$$E_j^l = |F_j^l|^2 .$$

There are two straightforward accumulations of the frequency information from the segments to represent the spectrum of the entire signal: summation of the complex components and summation of the energies.

First, complex, or "coherent," summation is defined by

$$\varphi_j = \sum_0^{L-1} F_j^l .$$

It can be shown that the  $\varphi_j$  are exact samples of the spectra  $F_m$  for the frequencies  $m$  such that  $m=jN$ . For these frequencies, the effect in the frequency domain of the exact phasing between eigenrays which occur in different segments of the record is preserved.

However, the spectral levels at the unsampled frequencies  $m$  such that  $jN < m < jN+N$  do not contribute to the spectrum as estimated via coherent summation. One consequence of this is that Parseval's relation is not preserved. This "coherent" summation has an extra advantage that the order of summation and transformation may be reversed. The energy in interval  $[F_1, F_2]$  as estimated via coherent summation would be

$$\epsilon_{12} = \sum_{j=j_1}^{j_2} |\varphi_j|^2 ,$$

with

$$j_1 = \frac{f_1}{L\Delta t} , \quad j_2 = \frac{f_2}{L\Delta t} .$$

An alternative to the complex accumulation is summation of energies, or "incoherent" summation. Under this scheme, the energy  $\hat{E}_j$  at frequency  $j$  is given by

$$\hat{E}_j = \sum_{l=0}^{L-1} E_j^l .$$

It can be shown that Parseval's relation is preserved under this definition. Unlike the complex summation, the spectral levels at the unsampled frequencies,  $jN < m < jN + N$ , do contribute to  $\hat{E}_j$ ; the details of this interpolation are not easily described. However, the phasing between eigenrays in different segments of the record has no effect upon  $E_j$ .

#### B. Effects of Data Segment Length on Digital Signal Summation

It is anticipated that the two summation methods would begin to differ with increasing magnitude as the number of data segments is increased, by decreasing the size of each segment of a given detected shot signal. This is illustrated by an example involving three received shot signals. The first two signals are shown in Fig. 7 where the upper trace corresponds to hydrophone 2 and the lower trace corresponds to hydrophone 3 of the ACODAC system deployed at Site D of the CHURCH GABBRO propagation experiment. The signals shown here were received with hydrophones 2 and 3 with the explosive source 206 nm away. The ACODAC time was day 9, hour 20, minute 14, second 30 (8 December 1972, 0814).

The length of the shortest data segment is 512 samples, which corresponds to a time interval of 0.85 sec at a sample rate of 600 Hz. The total interval of the shot analyzed for its power in the 1/3 octave frequency band centered at 50 Hz is  $32 \times 512 = 16384$  samples (27.2 sec). In the most extreme case a total of 32 continuous segments (0.85 sec each) were Fourier transformed and summed coherently and incoherently. In the least extreme case the entire 16384 samples (27.2 sec) were transformed as one record. Between these two extremes the number of data segments used were 2, 4, 8, and 16 (13.6, 6.8, 3.4, and 1.7 sec each respectively).

The reference for the comparison of the coherent and incoherent summations is the output of a digital recursive filter with Butterworth

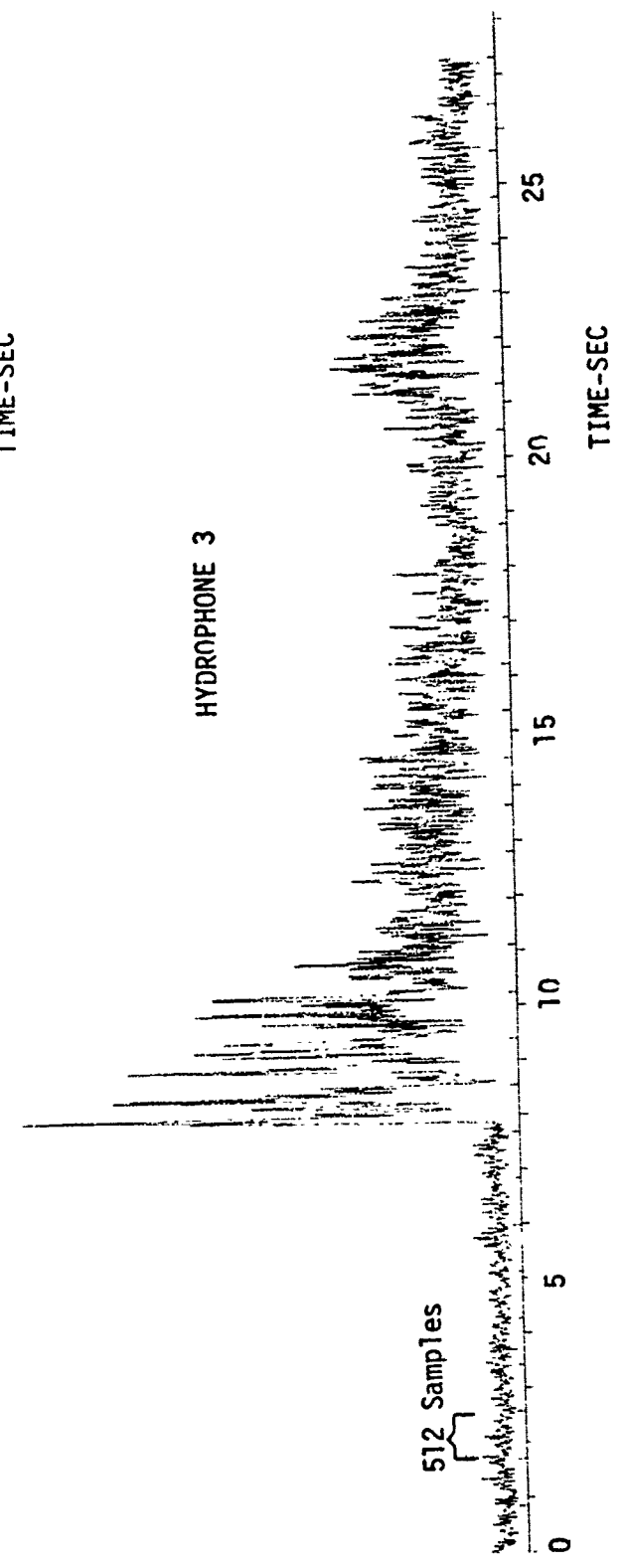
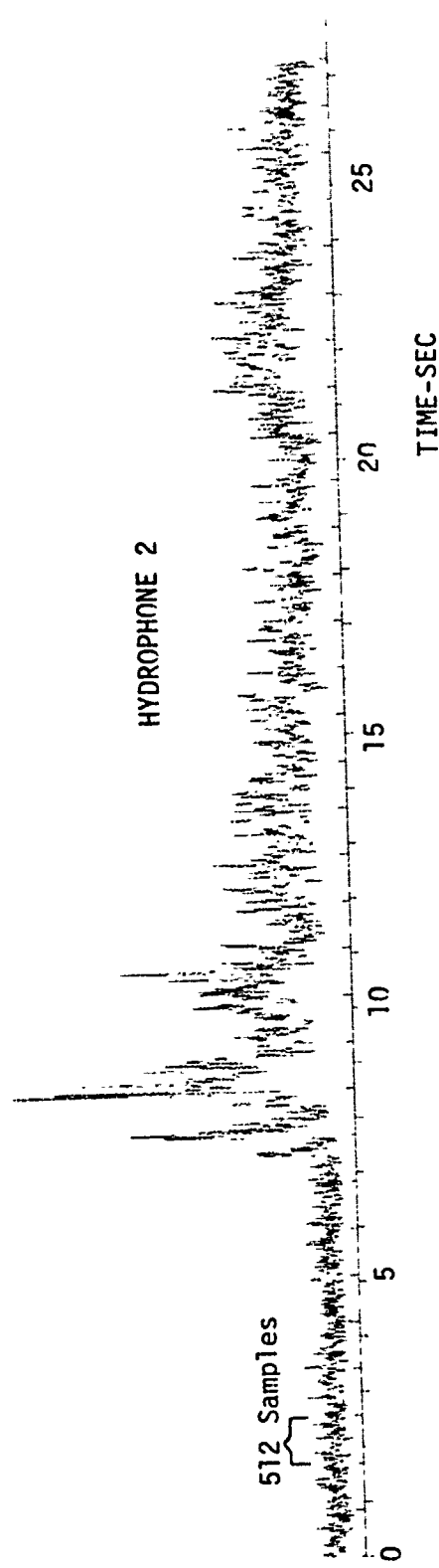


FIGURE 7  
SHOT SIGNALS USED TO COMPARE ENERGY COMPUTATIONS

filter characteristics. In the example shown here a 6-pole Butterworth filter was selected to match analog filters previously used for the analysis of ACODAC data.

The frequency response of the recursive filter, shown in Fig. 8, was computed by generating sine waves of varying frequency and measuring the output power. The impulse response was also computed and is plotted in Fig. 9.

Figure 10 shows both the coherent and incoherent energy summations as a function of the number of segments transformed. The coherent summation begins to diverge from the reference energy as the number of segments increases. When the number of data segments is 32, (each segment 0.85 sec) the percentage error, defined as

$$\text{Percentage Error} = \frac{|\text{summed energy} - \text{reference energy}|}{\text{reference energy}} 100 \quad ,$$

is 28%. The corresponding decibel error is

$$\text{Decibel Error} = 10 \log \frac{\text{summed energy}}{\text{reference energy}} = -1.4 \text{ dB.}$$

Whenever four segments are used, the corresponding errors are 1.6% and -0.01 dB. Note that the incoherent summation gives energy values very close to the reference energy. Figure 11 has the corresponding error analysis for the received signal from hydrophone 3. For the coherent summation case, the fluctuations with increasing rms levels will occur as the size of the segment is decreased, and these errors will appear as larger deviations, either positive or negative, about the true power spectrum. Thus, if other shot signals were analyzed in this manner, it is expected that the magnitude of the error would be similar, for a given segment size, but that the error would be either positive or negative. This fluctuation about the true power spectrum can be seen by comparing Figs. 10 and 11. Note again that

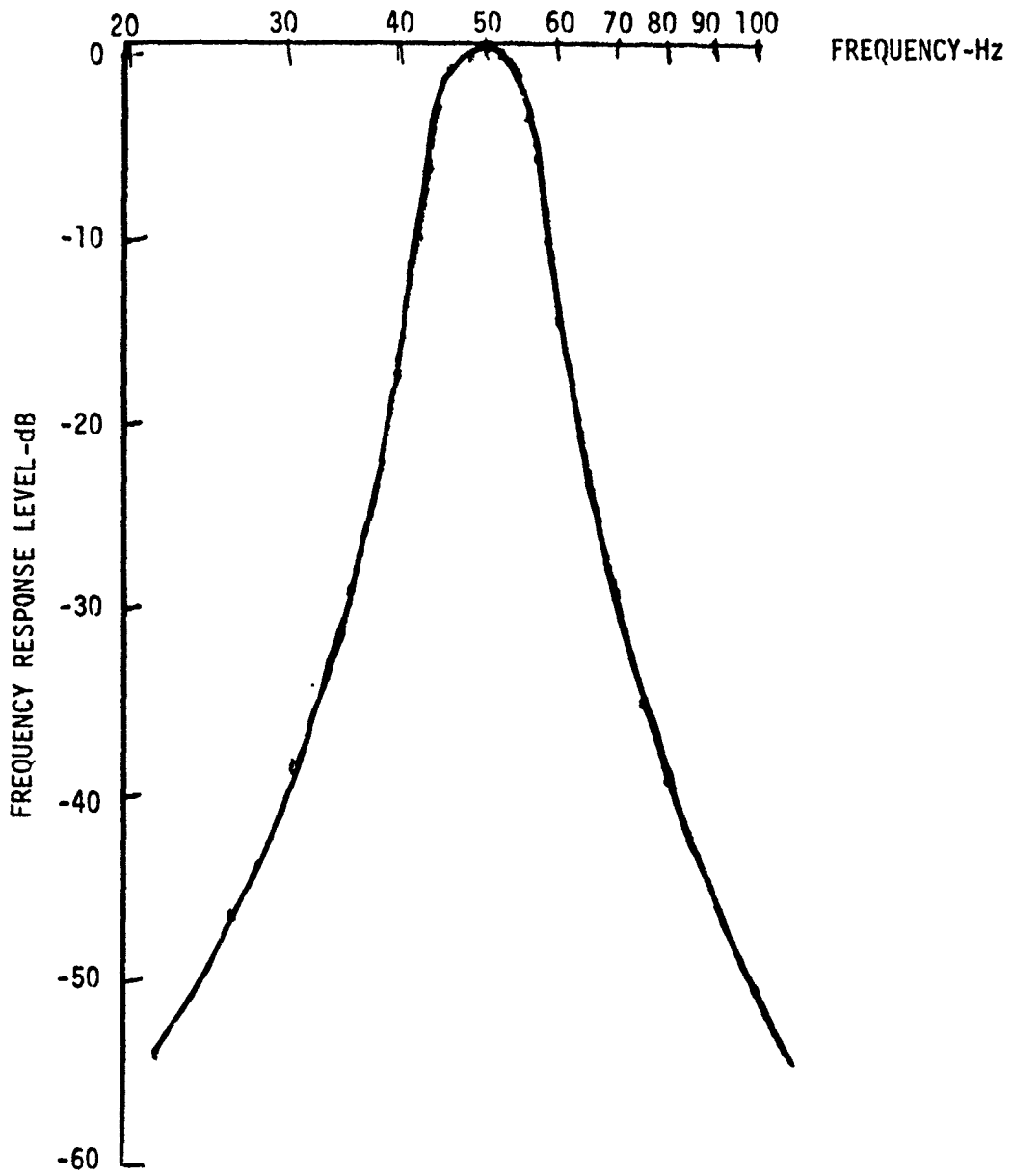


FIGURE 8  
FREQUENCY RESPONSE OF 1/3 OCTAVE  
RECURSIVE FILTER  
(6-POLE BUTTERWORTH)



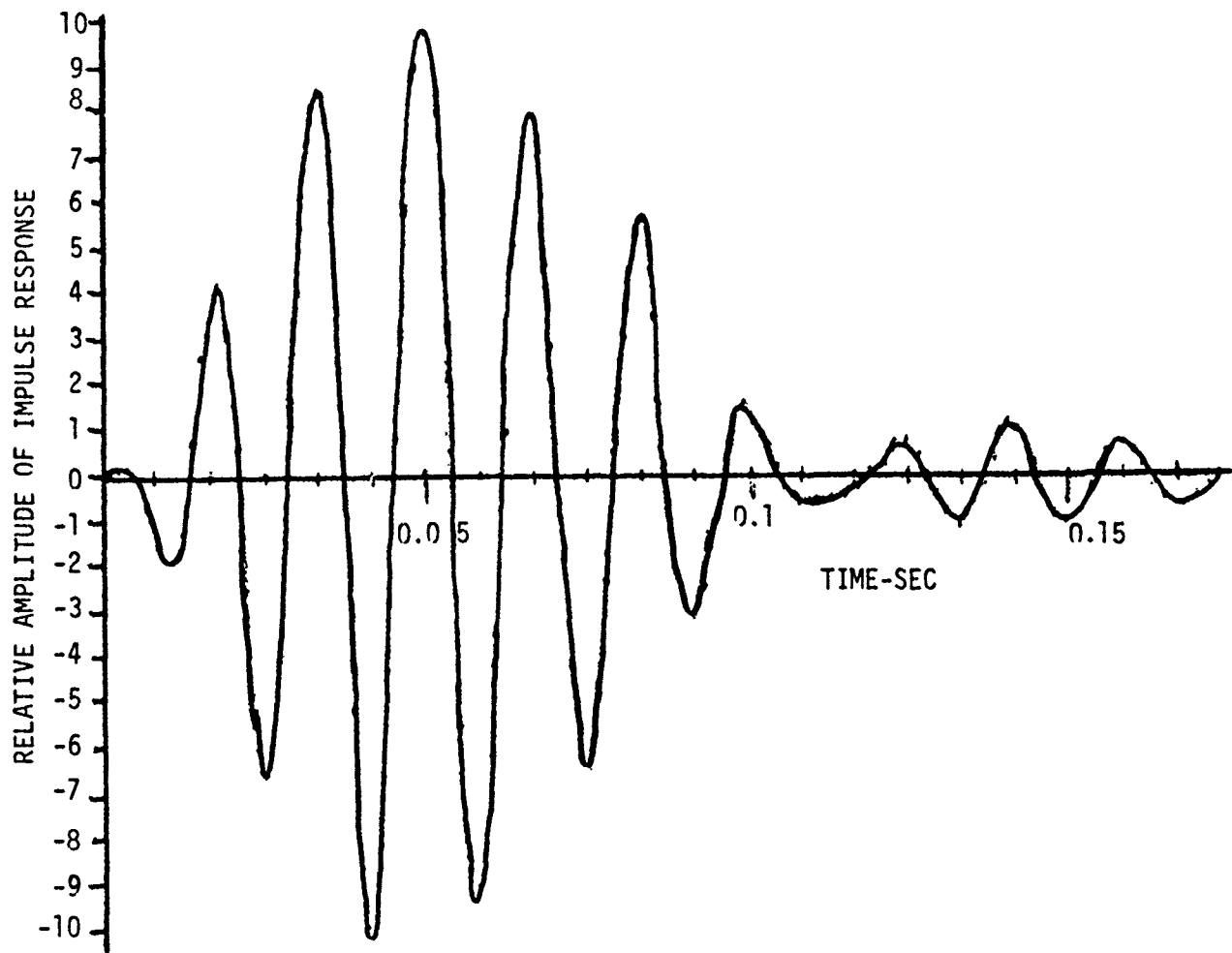


FIGURE 9

IMPULSE RESPONSE OF 1/3 OCTAVE RECURSIVE FILTER  
WHOSE FREQUENCY RESPONSE IS SHOWN IN FIGURE 8

(6 POLE BUTTERWORTH)

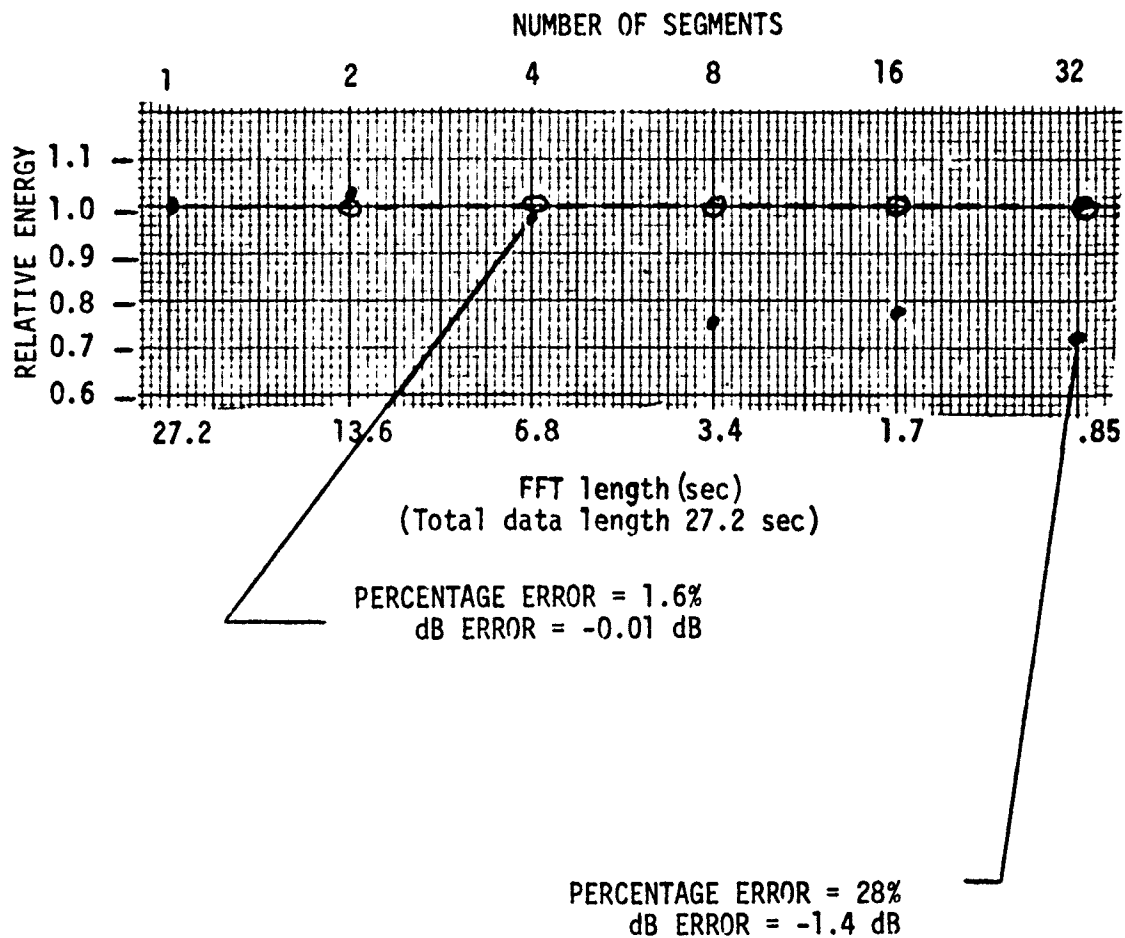


FIGURE 10

COMPARISON OF 1/3 OCTAVE BAND ENERGIES  
OBTAINED BY COHERENT AND INCOHERENT SUMMATION

SHOT 1: CHURCH GABBRO HYDROPHONE 2

FREQUENCY RANGE: 44.5-56.1 Hz

---REFERENCE LEVEL

...COHERENT SUMMATION

ooo INCOHERENT SUMMATION

SIGNAL-TO-NOISE RATIO OF FILTERED SHOT  $\approx 7$  dB

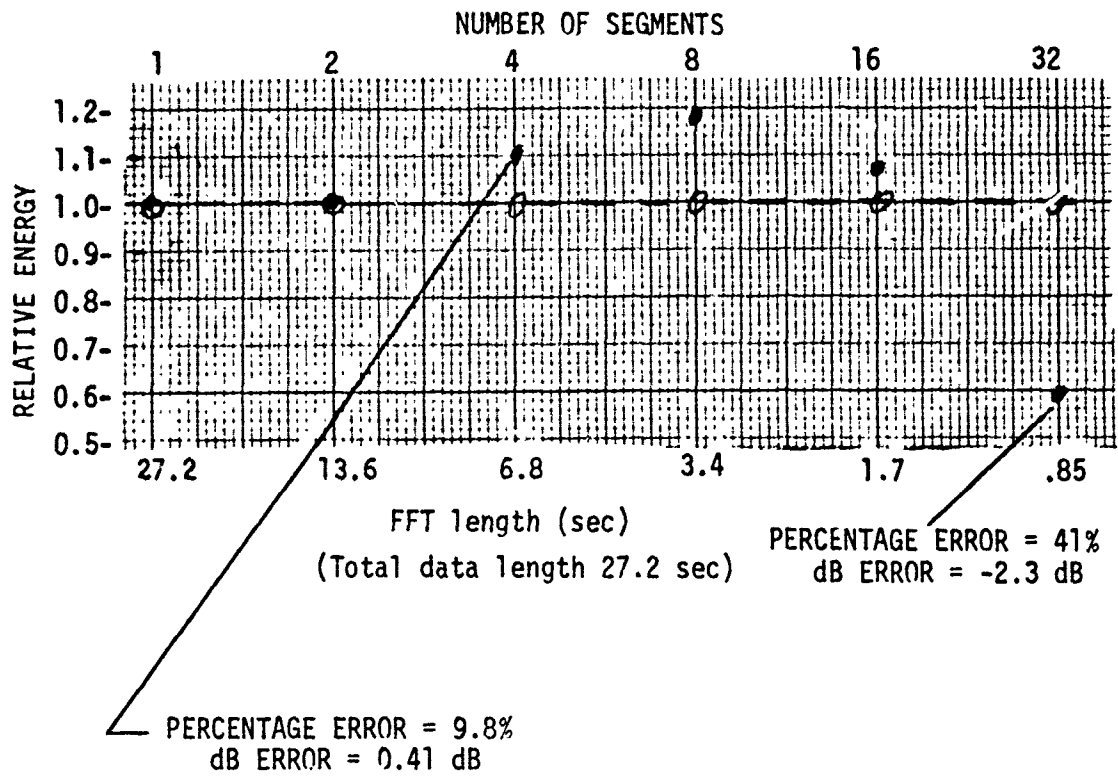


FIGURE 11  
 COMPARISON OF 1/3 OCTAVE BAND ENERGIES OBTAINED  
 BY COHERENT AND INCOHERENT SUMMATION  
 SHOT 1: CHURCH GABBRO HYDROPHONE 3  
 FREQUENCY RANGE: 44.5-56.1 Hz  
 --- REFERENCE LEVEL  
 ... COHERENT SUMMATION  
 OOO INCOHERENT SUMMATION  
 SIGNAL-TO-NOISE RATIO OF FILTERED SHOT  $\approx$  7 dB

incoherent summation gives results essentially equivalent to the reference level for any number of segments up to 32. From these results it may be concluded that, for data of this type, the loss of phase coherence (incoherent summation) between record segments causes less error than does the loss of information at unsampled frequencies (coherent summation). The agreement between the incoherent summation and the reference suggests that there is no critical phasing among components of the signal separated by more than a few seconds.

One further point was made with these two shot signals (Fig. 7). In a practical situation the received shot signal is never known exactly due to the influence of background noise (ambient or system). A question arises concerning the effect that an ambiguity in shot location has on the estimation of the energy in a given frequency band with coherent or incoherent summation. Some insight is obtained by considering Fig. 12, which is identical to Fig. 7 except that the beginning of the defined shot is earlier by a time of approximately 3.5 sec. Analyzing this signal in precisely the same manner as the previous example (Figs. 10 and 11) the data in Figs. 13 and 14 were generated. As can be seen the effect of not knowing the epoch exactly resulted in approximately 0.1 dB difference in the estimation of the shot energy by coherent or incoherent summation. It is expected, however, that the ambiguity in epoch will have more serious consequences as the signal-to-noise ratio of the shot decreases to a relatively lower level.

The recorded shot signals shown in Fig. 7 do not exhibit any strong multipath structure which conceivably could yield different results with respect to the comparisons of coherent and incoherent summations. A signal with a strong multipath structure evident is shown in Fig. 15. This signal was received with hydrophone 2 of the ACODAC system located at Site D with a range of 104 nm from the source. The ACODAC time was day 10, hour 7, minute 23, second 10. A comparison

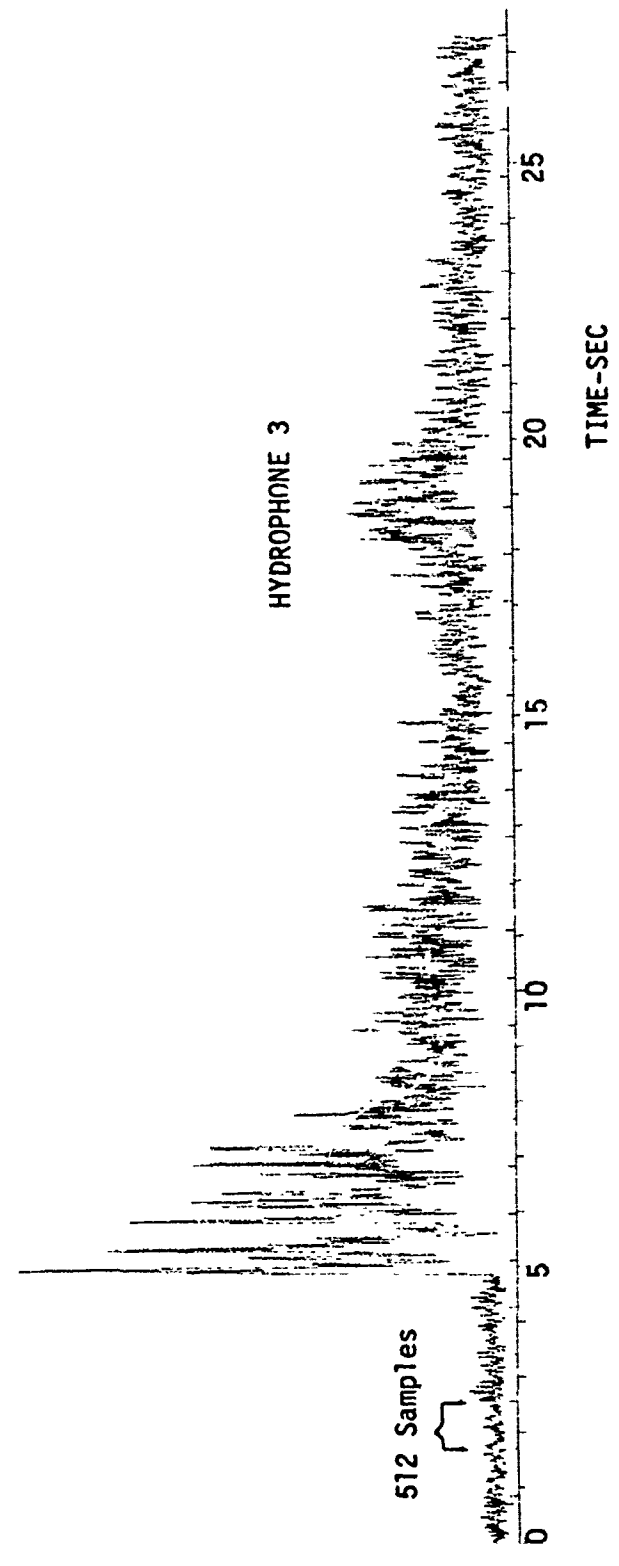
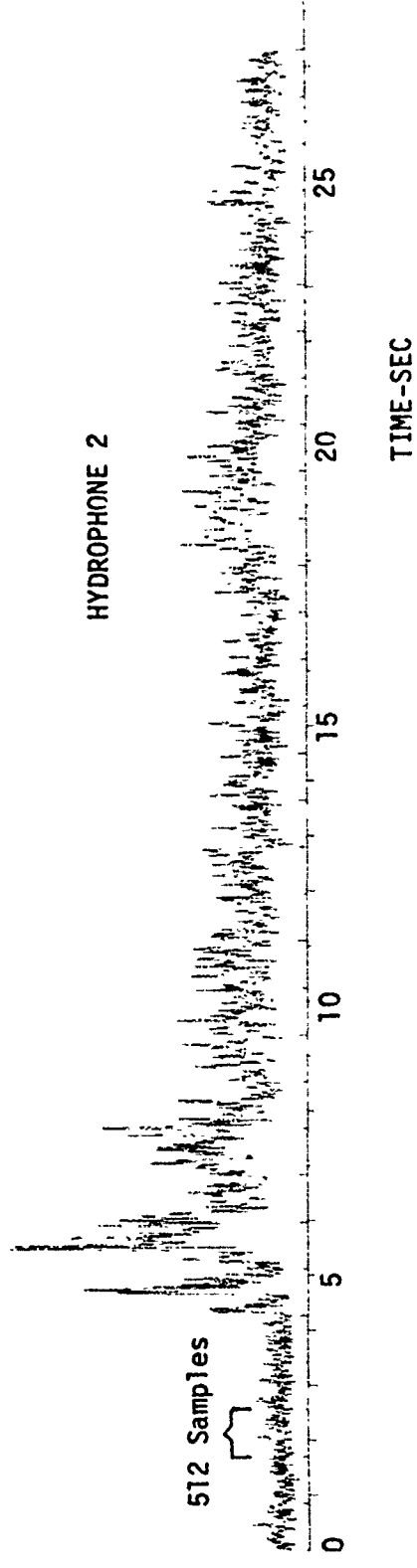


FIGURE 12  
SHOT SIGNALS USED TO COMPARE ENERGY COMPUTATIONS

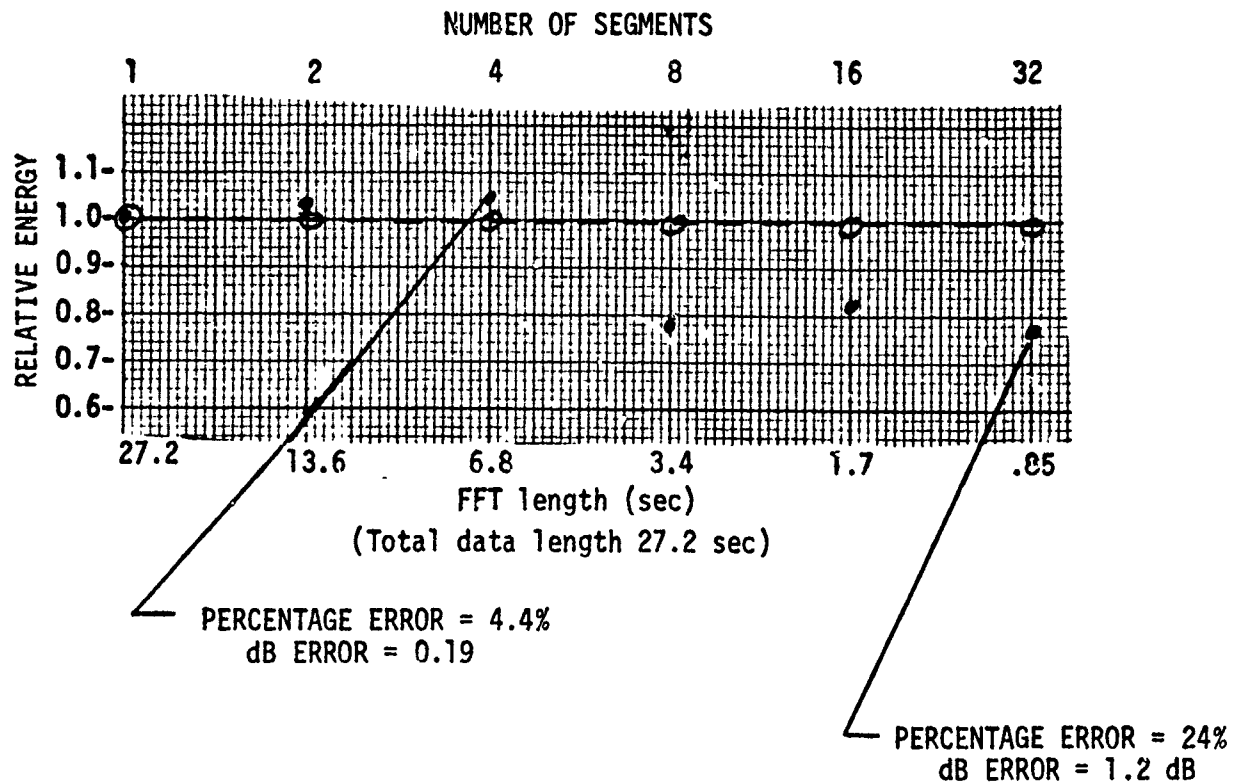


FIGURE 13

COMPARISON OF 1/3 OCTAVE BAND ENERGIES OBTAINED  
 BY COHERENT AND INCOHERENT SUMMATION  
 SHOT 2: CHURCH GABBRO HYDROPHONE 2  
 FREQUENCY RANGE: 44.5-56.1 Hz  
 ----REFERENCE LEVEL  
 ... COHERENT SUMMATION  
 OOO INCOHERENT SUMMATION  
 SIGNAL-TO-NOISE RATIO OF FILTERED SHOT  $\approx$  7 dB

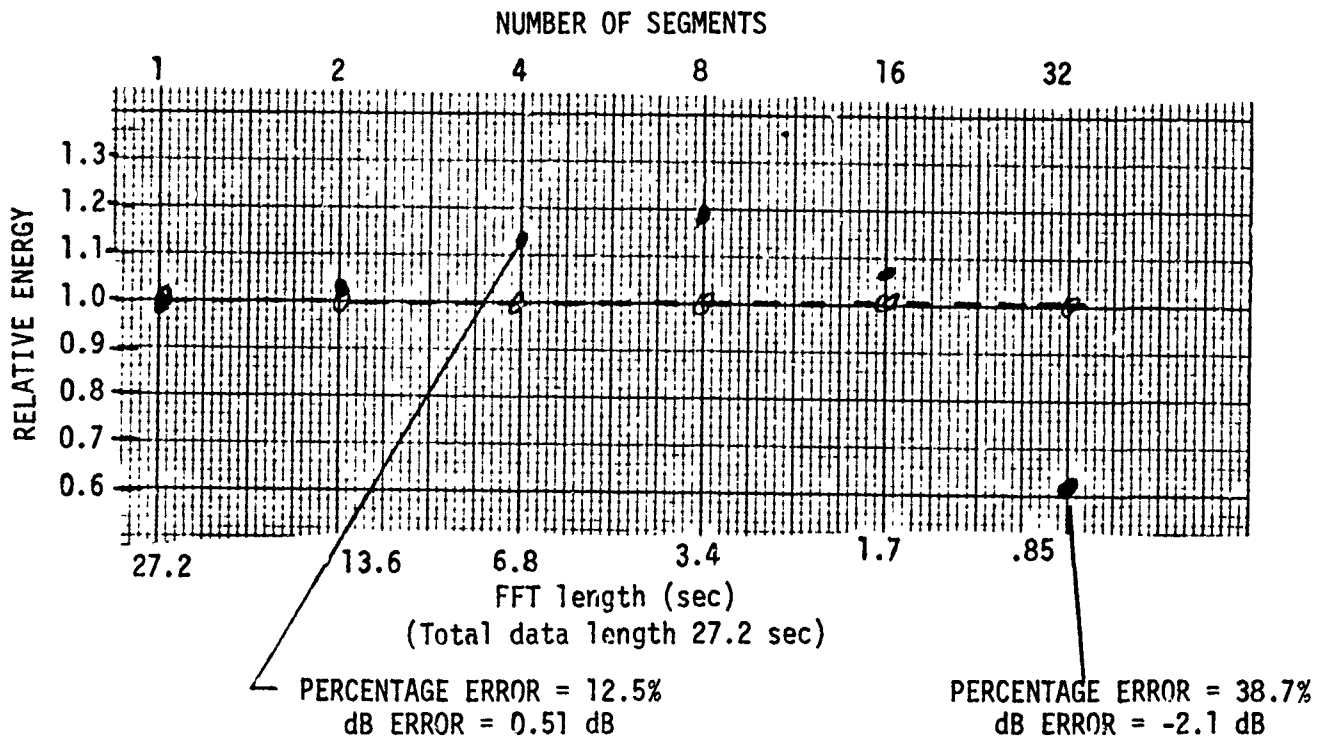


FIGURE 14  
 COMPARISON OF 1/3 OCTAVE BAND ENERGIES OBTAINED  
 BY COHERENT AND INCOHERENT SUMMATION  
 SHOT 2: CHURCH GABBRO HYDROPHONE 3  
 FREQUENCY RANGE: 44.5-56.1 Hz  
 --- REFERENCE LEVEL  
 ... COHERENT SUMMATION  
 ooo INCOHERENT SUMMATION  
 SIGNAL-TO-NOISE RATIO OF FILTERED SHOT  $\approx$  7 dB

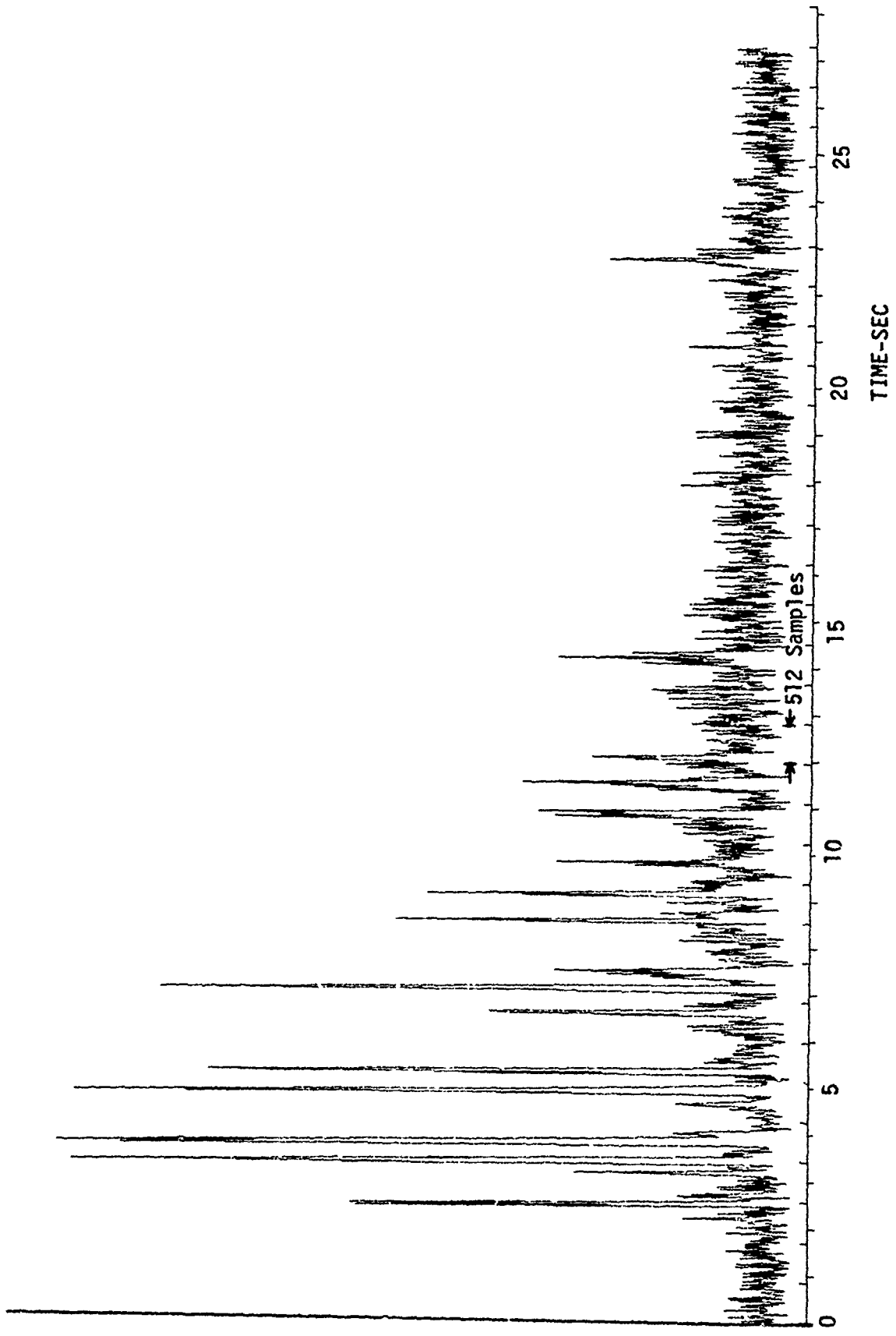


FIGURE 15  
SHOT SIGNAL USED TO COMPARE ENERGY COMPUTATIONS

SIGNAL LEVEL

AS-74-380



of the coherent and incoherent energies in the one-third octave band at 50 Hz is shown in Fig. 16, and the errors are of the same magnitude as those of the shots with the fused multipath structure.

### C. Comparison of Methods of Digital Signal Summation

For the first ACODAC shot analysis performed at ARL, both the coherent and incoherent summation results were included. These preliminary data from approximately 700 shots allow a statistical comparison of the two techniques.

The first experimental data are summarized in Tables I and II (ACODAC hydrophones 4 and 5, respectively) where the means and variances of signal-plus-noise (S+N) and signal-to-noise ratios  $(S+N)/\hat{N}$  corresponding to several one-third octave frequency bands are listed for both coherent and incoherent summation methods. Also listed are the correlation coefficients (covariance) computed between the coherent and incoherent forms of these estimates.

To estimate the shot energy S, which one must do to compute propagation loss, the number (S+N) is first computed and from this is subtracted the noise estimate  $\hat{N}$ . Similarly the signal-to-noise ratio determines the accuracy of the estimates of important characteristics of the shot.

As an example of how the values of Tables I and II are computed, the mean of the coherent estimate of (S+N) (Table II) is

$$\text{MEAN}(S+N)_{\text{coh}}^f = \frac{1}{722} \sum_{i=1}^{722} (S+N)_{i,\text{coh}}^f$$

where  $(S+N)_{\text{coh}}^f$  is the estimated energy in a one-third octave band at the center frequency f. The sum is over 722 received shot signals. The shots were distributed with respect to the number of 4096 sample

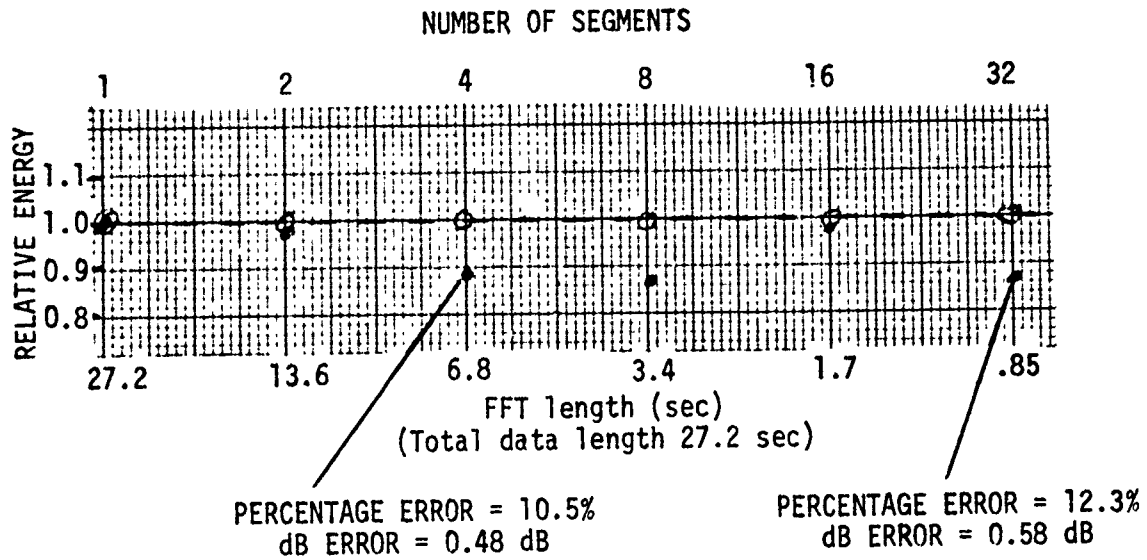


FIGURE 16

COMPARISON OF 1/3 OCTAVE BAND ENERGIES  
 OBTAINED BY COHERENT AND INCOHERENT SUMMATION  
 THE SHOT ANALYZED IS SHOWN IN FIGURE 15  
 FREQUENCY RANGE: 50 Hz

--- REFERENCE LEVEL  
 ... COHERENT SUMMATION  
 000 INCOHERENT SUMMATION

transforms as: 2 transforms, 38%; 4 transforms, 30%; 5 transforms, 21%; 6 transforms, 11%. Within a given shot the length of a basic time segment is 4096 samples (approximately 6.83 sec at 600 Hz sample rate). It is these contiguous time segments that are Fourier transformed and added coherently to obtain the spectrum of the one-third octave frequency band. These numbers from 722 shots are then averaged to give the mean of  $(S+N)$  according to the above expression.

The variance, likewise, is

$$\text{VAR}(S+N)_{\text{coh}}^f = \frac{1}{722} \sum_{i=1}^{722} \left[ (S+N)_{i,\text{coh}}^f - \text{MEAN}(S+N)_{\text{coh}}^f \right]^2$$

The correlation coefficient, computed to determine to what extent the coherent and incoherent sums are equivalent, is defined as (for the  $(S+N)$  estimate)

$$\text{COV}(S+N)^f = \frac{\frac{1}{722} \sum_{i=1}^{722} \left[ (S+N)_{i,\text{coh}}^f - M_{\text{coh}} \right] \left[ (S+N)_{i,\text{incoh}}^f - M_{\text{incoh}} \right]}{\left[ \text{VAR}_{\text{coh}}^f(S+N) \text{VAR}_{\text{incoh}}^f(S+N) \right]^{1/2}}$$

where  $M_{\text{coh}}$  and  $M_{\text{incoh}}$  are the corresponding means of  $(S+N)$ , coherent and incoherent. For the  $(S+N)/N$  estimates, the covariance was computed with data expressed in decibels. As can be seen, the covariance is normalized by the variances of the estimates. Thus, the maximum covariance is unity, a value which occurs if the coherent and incoherent techniques are identical.

As Tables I and II illustrate, the coherent and incoherent summation techniques are essentially identical in that most of the covariances are very close to unity, the majority being greater than 0.99. The lowest value is 0.9249, which is the covariance between the coherent and incoherent estimates of  $(S+N)/N$  in the one-third octave frequency

TABLE I

STATISTICS COMPARING COHERENT AND INCOHERENT TECHNIQUES FOR ESTIMATING  
POWER SPECTRA IN VARIOUS 1/3 OCTAVE FREQUENCY BANDS

DATA: 722 SHOTS; ACODAC HYDROPHONE 4

FREQUENCY	MEAN (COHERENT)	VARIANCE (COHERENT)	MEAN (INCOHERENT)	VARIANCE (INCOHERENT)	CORRELATION BETWEEN COHERENT AND INCOHERENT
12.5	0.0017	0.0094	0.0017	0.0101	0.9951
25	0.0147	0.0337	0.0145	0.0317	0.9971
50	0.0172	0.0135	0.0170	0.0131	0.9845
100	0.0031	0.0031	0.0039	0.0039	0.9972
160	0.0020	0.0061	0.0020	0.0060	0.9999
200	0.0025	0.0084	0.0025	0.0082	0.9999
TOTAL	0.1105	0.1358	0.1098	0.1342	0.9947
12.5	2.3096	3.3947	2.2309	3.6254	0.9403
25	4.9619	4.2518	4.9286	4.3403	0.9730
50	1.4785	3.2475	1.4704	3.1338	0.9806
100	2.4530	3.2049	2.4352	3.2325	0.9925
160	1.5893	3.1518	1.5829	3.1984	0.9962
200	0.9474	3.1891	0.9340	3.1963	0.9966
TOTAL	2.3505	4.1517	2.3221	4.2808	0.9947

N+S

N/(N+S)

TABLE II

STATISTICS COMPARING COHERENT AND INCOHERENT TECHNIQUES FOR ESTIMATING  
POWER SPECTRA IN VARIOUS 1/3 OCTAVE FREQUENCY BANDS

DATA: 721 SHOTS; ACODAC HYDROPHONE 5

<u>FREQUENCY</u>	<u>MEAN (COHERENT)</u>	<u>VARIANCE (COHERENT)</u>	<u>MEAN (INCOHERENT)</u>	<u>VARIANCE (INCOHERENT)</u>	<u>CORRELATION BETWEEN COHERENT AND INCOHERENT</u>
12.5	0.1636	0.3597	0.0654	0.3823	0.9968
25	0.4521	1.0196	0.4441	0.9318	0.9942
50	0.5299	0.4399	0.5506	0.4536	0.9765
100	0.1106	0.1242	0.1106	0.1277	0.9962
160	0.1704	0.2091	0.1714	0.2180	0.9886
200	0.0939	0.1869	0.0934	0.1804	0.9993
TOTAL	3.6118	5.2374	3.5894	5.1968	0.9952
12.5	1.8009	3.0775	1.7568	3.2147	0.9249
25	3.8839	3.5477	3.9413	3.7106	0.9599
50	0.8119	2.9743	0.7880	2.9462	0.9772
100	0.8065	2.6416	0.8182	2.6688	0.9836
160	0.0155	2.7035	-0.0039	2.8401	0.9721
200	-0.0034	3.0135	-0.0074	3.0252	0.9949
TOTAL	1.4633	3.4534	1.4412	3.5979	0.9923

34  
N+S

N/(N+S)

interval centered at 12.5 Hz. Further evidence of the similarity of the coherent and incoherent summations is given by the relative closeness of the corresponding means of the estimates of  $(S+N)$  and  $(S+N)/N$  and the similarities seen in the corresponding variances.

In connection with this study a large quantity of shot data was analyzed to obtain histograms of the quantities  $10 \log[(S+N)_{\text{coh}}/(S+N)_{\text{incoh}}]$  and  $10 \log[(S+N-\hat{N})_{\text{coh}}/(S+N-\hat{N})_{\text{incoh}}]$ , where  $S+N-\hat{N}$  is essentially the propagation loss of the explosive signal. The number  $\hat{N}$  is an estimate of the background noise. These histograms revealed that

1. the ensemble means of the quantities were mostly 0.1 dB or less; usually 0.01 dB for  $(S+N)$ , 0.1 for  $(S+N-\hat{N})$ . That is to say  $( )_{\text{coh}}$  is an unbiased estimate of  $( )_{\text{incoh}}$ .
2. The rms difference varied with frequency and integration time and were usually less than 1 dB.

#### IV. EFFECTS OF SAMPLING WITHOUT PHASE CONTROL

Mechanical variations (in time) in both the recording and playback tape recorders used with the analog data can result in frequency deviations or an increase in bandwidth of the original acoustic data. These variations can be compensated for in part by the recording, simultaneously with the acoustic data, of a reference frequency track which is used on playback as a clock for the analog-to-digital conversion of the data. To demonstrate the effect of not compensating for the mechanical variations in the record-playback process, the power spectra of Figs. 17 and 18 are shown. Figure 17 shows the estimated power spectrum of the 100 Hz ACODAC calibration signal which was digitized with the 50 Hz signal of the time code channel as a reference clock (multiplied to 600 Hz). In contrast, Fig. 18 shows the corresponding power spectrum that is estimated from the calibration signal digitized without the benefit of the 50 Hz reference track. The spread in the spectrum due to the lack of phase control changes from approximately 0.1 Hz to approximately 0.3 Hz at the half power point, illustrating the requirement of a reference track to compensate for the mechanical variations in the tape recording-playback process.

Preceding Page Blank

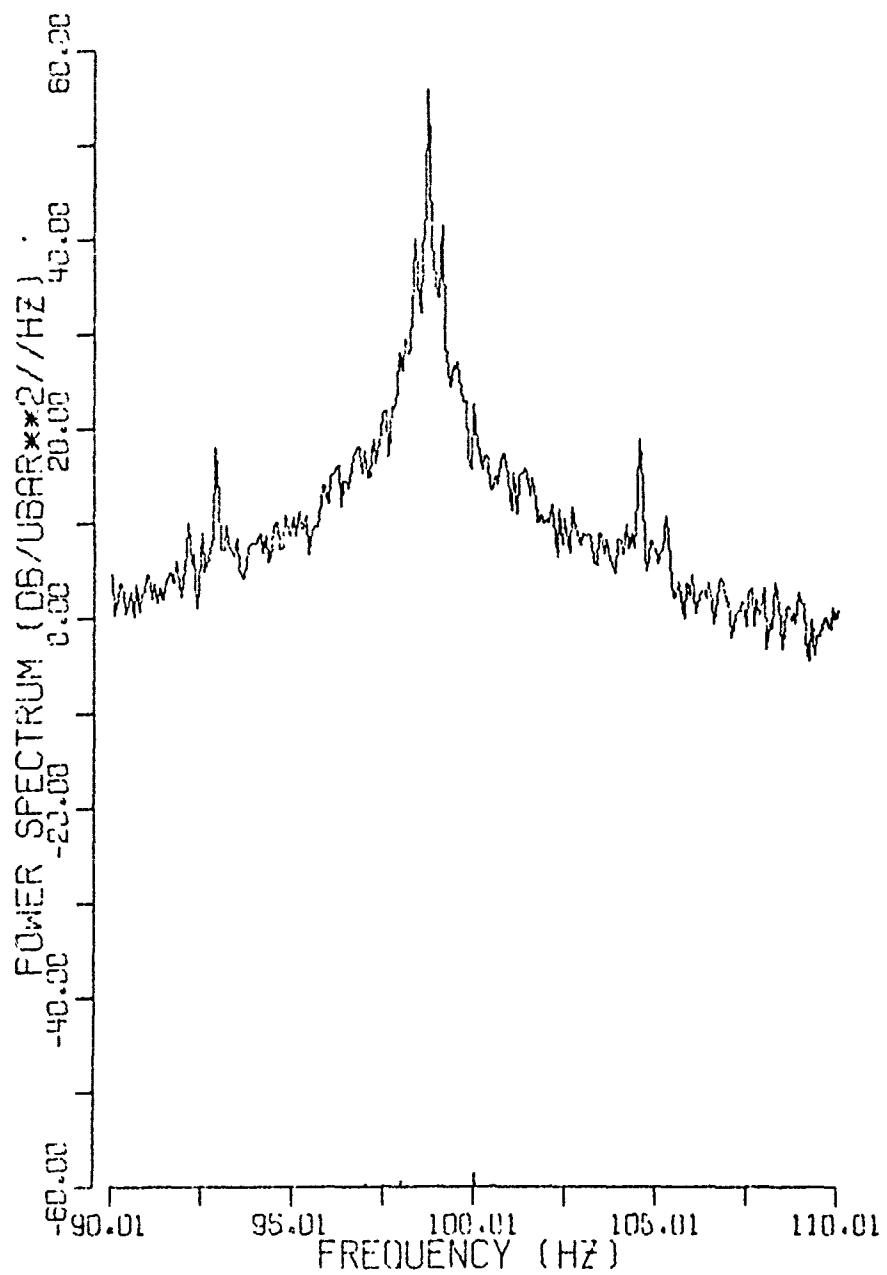


FIGURE 17  
 POWER SPECTRUM OF 100 Hz CALIBRATION SIGNAL  
 DIGITIZED WITH PHASE CONTROL

AS-74-382



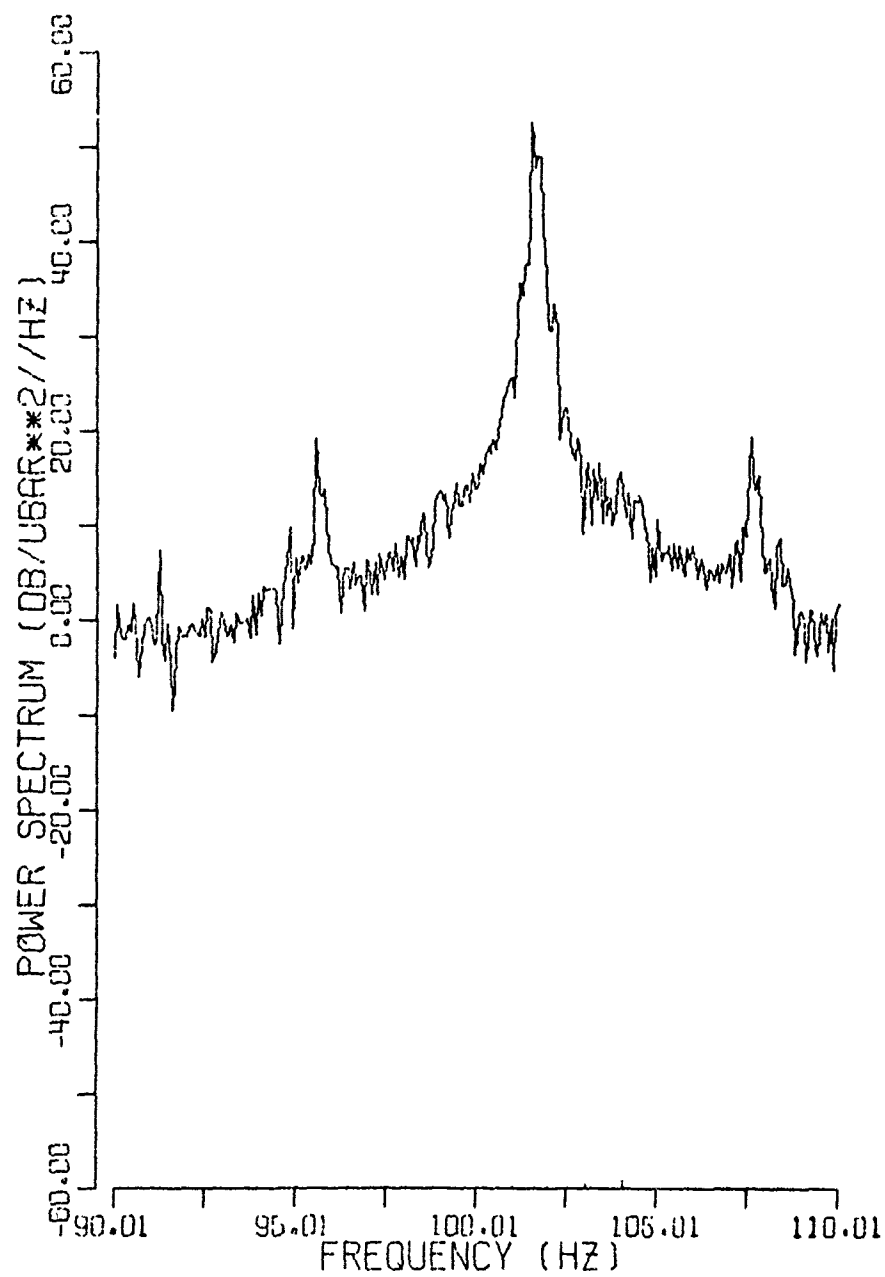


FIGURE 18  
POWER SPECTRUM OF 100 Hz CALIBRATION  
SIGNAL DIGITIZED WITHOUT PHASE CONTROL

## V. STABILITY OF CALIBRATION SIGNAL AS A FUNCTION OF TIME

The calibration signals are an integral part of the ACODAC system and their stability during the course of a recording period is a prerequisite for the accurate estimation of the received acoustical energy. For this reason the calibration signals of a CHURCH GABBRO tape were checked for energy stability over a 24 h period. To accomplish this, five 3.6 min calibration segments, with a separation of 6 h between two successive segments, were digitized at a sample rate of 600 Hz. This was done for both the 50 Hz and 200 Hz calibration signals on hydrophones 4, 5, and 6. In addition, this was done on two SUS runs.

Once in digital form, the energies of each 3.6 min data segment in one-third octave bands about the center frequencies (50 and 200 Hz) were computed. The results are summarized in Table III, which shows relative powers, expressed in decibels. The results shown here indicate that the calibration signal is very stable; a typical variation in power over a 24 h period is of the order 1 dB.

**Preceding Page Blank**

TABLE III

## STABILITY OF CHURCH GABBRO CALIBRATION SIGNALS

CH 4		CH 5		CH 6		
50 Hz	200 Hz	50 Hz	200 Hz	50 Hz	200 Hz	
55.6	55.1	56.7	52.0	56.9	54.1	
55.6	55.3	56.9	52.4	56.9	54.0	
55.5	54.8	56.7	51.9	56.7	53.6	
55.7	55.7	56.9	52.7	56.9	54.4	1st SUS Run
55.5	55.0	56.8	52.1	56.8	54.0	
47.3	44.2	44.2	38.5	45.7	42.3	
46.3	43.5	44.8	33.3	46.4	43.0	2nd SUS Run
45.8	42.7	44.4	38.7	45.9	42.4	

The numbers shown here are relative powers expressed in decibels.

## VI. SUMMARY

The data presented in this report describe the errors associated with the processing of the acoustical data obtained from the ACODAC receiving arrays and allow comparison of these errors with the fluctuations due to the variations of the acoustical environment (see Figs. 2 through 6). Specifically, it has been determined that

1. on a single ARL digitizing day, for repeated digitization, the energy in frequency bands for either shots or noise had standard deviations of 1 to 2%; the energy in the same bands of calibration signals showed a similar spread.

2. the signal levels as digitized showed variations from day to day which yielded 5 to 10% ( $5\% \approx 0.2$  dB) deviations of energy in the bands before the calibration signal was used for compensation;

3. the times at which the automatic shot processor detected a shot showed no fluctuations with repeated processing other than those to be expected from the temporal resolution imposed by the sampling rate (i.e., approximately 20 msec);

4. the standard deviations due to repeated processing of transmission loss for a given frequency band is of the order of 0.1 to 0.2 dB.

5. the ensemble means of the quantity  $10 \log \left[ \frac{(S+N-\hat{N})_{\text{coh}}}{(S+N-\hat{N})_{\text{incoh}}} \right]$  obtained from analysis of approximately 700 shots were of the order of 0.1 dB or less with a rms value of less than 1.0 dB; these numbers indicate the closeness of measuring transmission loss by either technique.

6. to prevent an introduction of frequency smearing due to mechanical variations in the recording and playback operations of the tape recorder, a reference track should be used in any processing of the data, whether analog or digital (see Figs. 17 and 18).

7. the stability of the ACODAC calibration signal is good as indicated by a variation in power of only 1 dB over a 24 h period (see Table III).

20 December 1973

DISTRIBUTION LIST FOR  
ARL-TM-73-42  
UNDER CONTRACT N00014-70-A-0166-0016

No. of Copies

1	Commanding Officer Office of Naval Research Department of the Navy Arlington, VA 22217 Attn: Code 102-OS
2	Code 102-OSC
1	AESD
1	Commander Naval Electronic Systems Command Department of the Navy Washington, D.C. 20360 Attn: PME-124/TA
1	Director Naval Research Laboratory Washington, D. C. 20375 Attn: Code 8160
1	Code 8168
1	Commander Naval Undersea Center San Diego, CA 92132 Attn: Code 502
1	Officer in Charge Naval Underwater Systems Center New London Laboratory New London, CT 06320 Attn: Code TA
1	Commander U. S. Naval Oceanographic Office Department of the Navy Washington, D.C. 20390 Attn: Code 6160
1	Director Marine Physical Laboratory Scripps Institution of Oceanography San Diego, CA 92152 Attn: Dr. G. B. Morris

Distribution List for ARL-TM-73-42 under Contract N00014-70-A-0166-0016  
(Cont'd)

No. of Copies

12	Commanding Officer and Director Defense Documentation Center Defense Services Administration Cameron Station, Building 5 5010 Duke Street Alexandria, VA 22314
1	Commanding Officer Office of Naval Research Branch Office Chicago 536 South Clark Street Chicago, IL 60605
1	University of Miami School of Marine and Atmospheric Sciences 10 Rickenbacker Causeway Miami, FL 33149 Attn: Dr. S. C. Daubin
1	Woods Hole Oceanographic Institution Woods Hole, MA 02543 Attn: Dr. E. E. Hays
1	Dr. R. W. Nowak
	Atlantic Oceanographic and Meteorological Laboratories National Oceanic and Atmospheric Adm. 15 Rickenbacker Causeway Miami, FL 33149 Attn: Dr. J. Proni
	Arthur D. Little, Inc. 15 Acorn Park Cambridge, MA 02140 Attn: Mr. D. L. Sullivan
1	B-K Dynamics, Inc. 2351 Shady Grove Road Rockville, MD 20850
1	Attn: Mr. A. E. Fadness
1	Mr. P. G. Bernard
1	Undersea Research Corporation 1920 Aline Avenue Vienna, VA 22180 Attn: Mr. J. A. Hess

Distribution List for ARL-TM-73-42 under Contract N00014-70-A-0166-0016  
(Cont'd)

No. of Copies

1	Underwater Systems, Inc 8121 Georgia Avenue Silver Spring, MD 20910 Attn: Dr. M. S. Weinstein
1	Hydrospace-Challenger, Inc. 2150 Fields Road Rockville, MD 20850 Attn: Mr. John Nardello
1	Office of Naval Research Resident Representative Room No. 582 Federal Building 300 East 8th Street Austin, TX 78701
1	Aubrey L. Anderson, ARL/UT
1	Karl C. Focke, ARL/UT
1	Loyd D. Hampton, ARL/UT
1	Stephen K. Mitchell, ARL/UT
1	Terry D. Plemons, ARL/UT
1	Jack A. Shooter, ARL/UT
1	Steven L. Watkins, ARL/UT
1	Library, ARL/UT
10	ARL Reserve



UNCLASSIFIED

SECURITY CLASSIFICATION OF THIS PAGE (When Data Entered)

REPORT DOCUMENTATION PAGE		READ INSTRUCTIONS BEFORE COMPLETING FORM
1. REPORT NUMBER ARL-TM-73-42	2. GOVT ACCESSION NO.	3. RECIPIENT'S CATALOG NUMBER
4. TITLE (and Subtitle) QUALITY CONTROL ANALYSIS OF SUS PROCESSING FROM ACODAC DATA		5. TYPE OF REPORT & PERIOD COVERED technical memorandum
		6. PERFORMING ORG. REPORT NUMBER
7. AUTHOR(s) Stephen K. Mitchell and Terry D. Plemons		8. CONTRACT OR GRANT NUMBER(s) N00014-70-A-0166, Task 0016
9. PERFORMING ORGANIZATION NAME AND ADDRESS Applied Research Laboratories The University of Texas at Austin Austin, Texas 78712		10. PROGRAM ELEMENT, PROJECT, TASK AREA & WORK UNIT NUMBERS
11. CONTROLLING OFFICE NAME AND ADDRESS Office of Naval Research Department of the Navy Arlington, Virginia 22217		12. REPORT DATE 20 Dec 1973
		13. NUMBER OF PAGES 47
14. MONITORING AGENCY NAME & ADDRESS (If different from Controlling Office)		15. SECURITY CLASS. (of this report) UNCLASSIFIED
		15a. DECLASSIFICATION/DOWNGRADING SCHEDULE
16. DISTRIBUTION STATEMENT (of this Report) Distribution limited to U. S. Government Agencies only, Test and Evaluation; 16 January 1974. Requests for this document must be referred to the Office of Naval Research, Code 102-05C.		
17. DISTRIBUTION STATEMENT (of the abstract entered in Block 20, if different from Report)		
18. SUPPLEMENTARY NOTES		
19. KEY WORDS (Continue on reverse side if necessary and identify by block number) Digital Spectral Analysis                      Phase Control Coherent Processing                              Calibration Signal Incoherent Processing                          Analog-to-Digital Conversion Error Analysis                                      Arrival Time Estimation Repeatability		
20. ABSTRACT (Continue on reverse side if necessary and identify by block number) The errors associated with the analysis of acoustic signals generated by underwater explosive sources are analyzed in this report. Thus, the effects of analog reproduction and subsequent digital conversion of the data on the estimation of propagation loss are considered. In addition the techniques of the spectral analysis as applied to these data are discussed. It is shown that the digitizing processing can be repeated on a day-to-day basis to the extent that the energy in frequency bands for either shots or noise have standard deviations of 1 to 2%. The times at which the automatic shot		

DD FORM 1473

1 JAN 73

EDITION OF 1 NOV 65 IS OBSOLETE  
S/N 0102-014-6601

UNCLASSIFIED

SECURITY CLASSIFICATION OF THIS PAGE (When Data Entered)



**DEPARTMENT OF THE NAVY**

OFFICE OF NAVAL RESEARCH  
875 NORTH RANDOLPH STREET  
SUITE 1425  
ARLINGTON VA 22203-1995

IN REPLY REFER TO:

5510/1  
Ser 321OA/011/06  
31 Jan 06

MEMORANDUM FOR DISTRIBUTION LIST

Subj: DECLASSIFICATION OF LONG RANGE ACOUSTIC PROPAGATION PROJECT  
(LRAPP) DOCUMENTS

Ref: (a) SECNAVINST 5510.36

Encl: (1) List of DECLASSIFIED LRAPP Documents

1. In accordance with reference (a), a declassification review has been conducted on a number of classified LRAPP documents.
2. The LRAPP documents listed in enclosure (1) have been downgraded to UNCLASSIFIED and have been approved for public release. These documents should be remarked as follows:

Classification changed to UNCLASSIFIED by authority of the Chief of Naval Operations (N772) letter N772A/6U875630, 20 January 2006.

DISTRIBUTION STATEMENT A: Approved for Public Release; Distribution is unlimited.

3. Questions may be directed to the undersigned on (703) 696-4619, DSN 426-4619.

A handwritten signature in black ink, appearing to read "B. F. Link".

BRIAN LINK  
By direction

Subj: DECLASSIFICATION OF LONG RANGE ACOUSTIC PROPAGATION PROJECT  
(LRAPP) DOCUMENTS

DISTRIBUTION LIST:

NAVOCEANO (Code N121LC – Jaime Ratliff)  
NRL Washington (Code 5596.3 – Mary Templeman)  
PEO LMW Det San Diego (PMS 181)  
DTIC-OCQ (Larry Downing)  
ARL, U of Texas  
Blue Sea Corporation (Dr. Roy Gaul)  
ONR 32B (CAPT Paul Stewart)  
ONR 321OA (Dr. Ellen Livingston)  
APL, U of Washington  
APL, Johns Hopkins University  
ARL, Penn State University  
MPL of Scripps Institution of Oceanography  
WHOI  
NAVSEA  
NAVAIR  
NUWC  
SAIC

## Declassified LRAPP Documents

Report Number	Personal Author	Title	Publication Source (Originator)	Pub. Date	Current Availability	Class.
WHOI73-59	Tollios, C. D.	THE ACODAC DATA PROCESSING SYSTEM	Woods Hole Oceanographic Institution	730901	AD0773114; ND	U
Unavailable	Russell, J. J.	DOCUMENTATION FOR COMPUTER PROGRAM SUMMARY: A COMPUTER PROGRAM TO SUMMARIZE SOUND SPEED PROFILE DATA	Naval Undersea Center	731001	AD0918907	U
MC001Vol2	Unavailable	CHURCH ANCHOR DATA ANALYSIS PLAN VOL 2 (U)	Maury Center for Ocean Science	731001	ND	U
73-9M7-VERAY-R2	Jones, C. H.	LRAPP VERTICAL ARRAY - PHASE III	Westinghouse Research Laboratories	731105	ADA001130; ND	U
55	Weinstein, M. S., et al.	SUS QUALITY ASSESSMENT	Underwater Systems, Inc.	731201	AD ND 45-875	U
ARL-TM-73-42	Mitchell, S. K., et al.	QUALITY CONTROL ANALYSIS OF SUS PROCESSING FROM ACODAC DATA	University of Texas, Applied Research Laboratories	731220	AD ND 00-283	U
Unavailable	Daubin, S. C.	CHURCH GABBRO TECHNICAL NOTE: CONTINUOUS CURRENT PROFILES	University of Miami, Rosenstiel School of Marine and Atmospheric Science	740101	AD0775333	U
Unavailable	Bitterman, D. S.	ACODAC AMBIENT NOISE SYSTEM	Woods Hole Oceanographic Institution	740101	ADA009440	U
ONR MC-002 VOL. 2; XONICS 885	Unavailable	LONG RANGE ACOUSTIC PROPAGATION PROJECT (LRAPP). SQUARE DEAL DATA ANALYSIS PLAN (U) VOLUME 2 - ANNEXES	Maury Center for Ocean Science; Xonics, Inc.	740101	ND	U
ARL-TM-74-12	Groman, R. O., et al.	SPECIAL HARDWARE FOR ARL ANALYSIS OF ACODAC DATA	University of Texas, Applied Research Laboratories	740314	ADA000295; ND	U
Unavailable	Unavailable	ASEPS NEAR FIELD TRANSMISSION LOSS MODIFICATION, P-2205	Ocean Data Systems, Inc.	740401	ADA096583	U
Report 001; MSAG-1	Unavailable	MEASUREMENT SYSTEMS ADVISORY GROUP	Office of Naval Research	740401	ADA096586; ND	U
ACR-196	Gregory, J. B.	PROJECT PACIFIC SEA SPIDER, TECHNOLOGY USED IN DEVELOPING A DEEP-OCEAN ULTRASTABLE PLATFORM	Office of Naval Research	740412	AD0529945; ND	U
Unavailable	Gottwald, J. T.	ANNUAL REPORT FOR 1 MAY 1973 - 30 APRIL 1974	Tracor, Inc.	740524	AD0920210	U
Unavailable	Unavailable	ACOUSTIC MODEL SUPPORT ACTIVITIES, P-2220	Ocean Data Systems, Inc.	740530	ADA096584	U
HCI-CMC-18540	Daubin, S. C.	TRANSMISSION LOSS OF LOW FREQUENCY UNDERWATER SOUND IN THE CAYMAN TROUGH (CHURCH GABBRO TECHNICAL NOTE)	University of Miami, Rosenstiel School of Marine and Atmospheric Science	740601	ADC000424; ND	U
HCI-CMC-18343	Daubin, S. C.	AMBIENT NOISE IN THE NORTHWEST CARIBBEAN SEA (CHURCH GABBRO TECHNICAL NOTE) (U)	University of Miami, Rosenstiel School of Marine and Atmospheric Science	740601	ND	U
Unavailable	Barnes, A., et al.	DISCRETE SHIPPING MODEL	Planning Systems, Inc.	740604	ND	U